SYNOPTIC CONTROL ON SNOW AVALANCHE ACTIVITY IN CENTRAL SPITSBERGEN

Holt Hancock[1,2], Jordy Hendrikx[3], Markus Eckerstorfer[4,5], Siiri Wickström[6]

[1]Department of Arctic Geology, University Centre in Svalbard, N-9171 Longyearbyen, Norway
5 [2]Department of Geosciences, University of Oslo, N-0371 Oslo, Norway
[3]Snow and Avalanche Lab, Department of Earth Sciences, Montana State University, P.O Box 173480, Bozeman, MT, 59717, USA
[4] Regional Climate Lab., Climate Department, NORCE Norwegian Research Centre, N-5838 Bergen, Norway
[5] Bjerknes Centre for Climate Research, N-5007 Bergen, Norway
10 [6] Department of Arctic Geophysics, University Centre in Svalbard, N-9171 Longyearbyen, Norway

Correspondence to: Holt Hancock (holt.hancock@unis.no)

Abstract

Atmospheric circulation exerts an important control on a region's snow avalanche activity by broadly determining the mountain weather patterns which influence snowpack development and avalanche release. In central Spitsbergen, the largest
15 island in the high-Arctic Svalbard archipelago, avalanches are a common natural hazard throughout the winter months. Previous work has identified a unique snow climate reflecting the region's climatically dynamic environmental setting but has not specifically addressed the synoptic-scale control of atmospheric circulation on avalanche activity here. In this work, we investigate atmospheric circulation's control on snow avalanching in the Nordenskiöld Land region of central Spitsbergen by first constructing a four-season (2016/2017 – 2019/2020) regional avalanche activity record using observations available on a
20 database used by the Norwegian Water Resources and Energy Directorate (NVE). We then analyze the synoptic atmospheric conditions on days with differing avalanche activity situations. Our results show atmospheric circulation conducive to elevated precipitation, wind speeds, and air temperatures near Svalbard are associated with increased avalanche activity in Nordenskiöld Land, but different synoptic signals exist for days characterized by dry, mixed, and wet avalanche activity. Differing upwind conditions help further explain differences in the frequency and nature of avalanche activity resulting from these various
25 atmospheric circulation patterns. We further employ a daily atmospheric circulation calendar to help contextualize our results in the growing body of literature related to environmental change in this location. This work helps expand our understanding of snow avalanches in Svalbard to a broader spatial scale and provides a basis for future work investigating the impacts of environmental change on avalanche activity in Svalbard and other locations where avalanche regimes are impacted by changing climatic and synoptic conditions.

1 Introduction

Snow avalanches are natural hazards occurring in mountainous environments where complex interactions between the terrain, weather, and snowpack allow for masses of snow to rapidly descend steep slopes (e.g. Schweizer et al., 2003a). Avalanche forecasts thus seek to reduce risks associated with snow avalanche hazards by predicting avalanche conditions by integrating

35   information related to an area's terrain, past and current meteorological conditions, and snowpack (LaChapelle, 1980; McClung, 2002b). Of the three factors – terrain, weather, and snowpack – contributing to avalanche release and considered in avalanche forecasts, terrain is generally considered static (e.g. Schweizer et al., 2003a), while the snowpack exhibits spatial heterogeneity which is difficult to resolve at broader spatial scales (Schweizer et al., 2008; Clark et al., 2011). Previous work investigating the controls on avalanching at broader, regional to sub-continental spatial scales has therefore focused on

40   understanding the linkages between synoptic-scale atmospheric circulation patterns and periods of increased avalanche activity (e.g. Birkeland et al., 2001; Fitzharris, 1987; Fitzharris and Bakkehøi, 1986; Keylock, 2003; Martin and Germain, 2017; Schauer et al., 2020).

The synoptic scale in meteorology refers to weather phenomena – such as extratropical cyclones – with horizontal extents on the order of 1000 km (e.g. Yarnal, 1993). Atmospheric processes at this scale are roughly analogous to a mountain range when

45   considering avalanche processes and related operational hazard forecasts (McClung, 2002b). As atmospheric circulation is the primary expression of meteorological conditions at this spatial scale, studying the interactions between atmospheric circulation and the surface environment is known as synoptic climatology (Yarnal, 1993). A synoptic avalanche climatology therefor relates a region's avalanche activity to synoptic-scale atmospheric circulation patterns and can serve as a basis for understanding – and thus forecasting for – avalanche activity at the regional scale. The foundation established by a synoptic

50   avalanche climatology represents the mean atmospheric conditions associated with avalanche activity in a particular location and provides a basis for considering the discrete meteorological conditions resulting from a specific synoptic event which lead to avalanche release.

Numerous studies have addressed avalanche activity at the synoptic scale through analyses of atmospheric circulation patterns. Synoptic avalanches climatologies have been developed for Iceland (Björnsson, 1980), the Norwegian mainland (Fitzharris

55   and Bakkehøi, 1986), western Canada (Fitzharris, 1987), the western United States (Birkeland et al., 2001; Schauer et al., 2020), the Spanish Pyrenees (García et al., 2009), Mt. Shasta in northern California (Hansen and Underwood, 2012), and portions of the northeastern United States (Martin and Germain, 2017). Other works investigating synoptic-scale meteorological controls on regional avalanche activity include analyses of the North Atlantic Oscillation's influence on the avalanche regimes in Iceland (Keylock, 2003) and the Eastern Pyrenees (García-Sellés et al., 2010) as well as the effects of

60   the El Niño Southern Oscillation on avalanche patterns in western Canada and Chile (McClung, 2013).

In the high-Arctic archipelago of Svalbard, atmospheric circulation classifications have been established through subjective (Niedźwiedź, 2013) and objective (Käsmacher and Schneider, 2011) classification methods. Previous work from this region

has utilized these classifications – primarily the subjective classification from Niedźwiedź (2013) – to relate atmospheric
circulation patterns to recent climatic warming across the archipelago (Isaksen et al., 2016), to analyze meteorological

65   conditions and snow distribution on select glacial systems (Laska et al., 2017; Małecki, 2015), and to characterize wintertime
rain-on-snow events (Wickström et al., 2020). Additional research on synoptic-scale meteorological processes in Svalbard
includes works examining the effects of atmospheric circulation on air temperatures (e.g. Bednorz and Fortuniak, 2011;
Bednorz and Kolendowicz, 2013), precipitation patterns (e.g. Serreze et al., 2015), cloudiness (Bednorz et al., 2016), and
extratropical cyclone activity (Rinke et al., 2017; Rogers et al., 2005; Wickström et al., 2019).

70   This study investigates the relation between atmospheric circulation patterns and avalanche activity in the Nordenskiöld Land
region of central Spitsbergen, the largest island in the Svalbard archipelago (Fig. 1). Spitsbergen is situated at the climatically
dynamic interface between the Arctic and North Atlantic regions where its proximity to poleward oceanic and atmospheric
heat transport pathways results in a warmer, wetter climate than expected at these latitudes. The West Spitsbergen Current off
the island's western coast – the northernmost extension of the warm Atlantic Gulf Stream – has a moderating effect on regional

75   temperatures and results in perennial ice-free conditions in the eastern Fram Strait (Walczowski and Piechura, 2011).
Atmospheric heat and moisture reach Svalbard during winter via extra-tropical cyclones traveling northeastwards along the
North Atlantic storm track, and temperatures can rise far above freezing, even in winter (e.g. Serreze et al., 2015; Vikhamar-
Schuler et al., 2016). Spatiotemporal fluctuations in sea-ice concentration and extent (e.g. Muckenhuber et al., 2016; Onarheim
et al., 2014), atmospheric and oceanic circulation (e.g. Cottier et al., 2007) and storm track location (e.g. Rogers et al., 2005;

80   Wickström et al., 2019) dramatically affect climatic and meteorological conditions in Spitsbergen, making the region one of
the most climatically sensitive in the world.

Nordenskiöld Land's high-Arctic maritime snow climate reflects central Svalbard's unique environmental setting (Eckerstorfer
and Christiansen, 2011a). Winter weather is characterized by prolonged periods of relatively cold, stable high pressure
interrupted by warmer, wetter low pressure systems traveling northwards along the North Atlantic storm track (Hanssen-Bauer

85   et al., 1990; Rogers et al., 2005). Wind slabs and ice layers form in the snowpack during these warm, wet winter storms and
are often separated by persistent weak layers of faceted grains developing during colder, stable periods (Eckerstorfer and
Christiansen, 2011a). Snow is readily transported by the wind across the region's broad plateau summits and expansive
glaciofluvial valleys in the absence of woody vegetation, and large cornices develop annually along the edges of the plateaus
(Vogel et al., 2012; Hancock et al., 2020). Avalanche activity in this environment is observed to cluster temporally in avalanche

90   cycles related to winter storms, where precipitation and strong winds result in modest snow fall amounts rapidly accumulating
in leeward areas (Eckerstorfer and Christiansen, 2011b). Although Nordenskiöld Land's winter climate and thin snowpack
promote persistent weak layer development throughout the season (Eckerstorfer and Christiansen, 2011a), the avalanche
regime here is nevertheless primarily direct action, with avalanches – even those releasing on deeper instabilities – typically
occurring in direct response to snow loading during winter storms (Eckerstorfer and Christiansen, 2011b, 2011c; Hancock et

95   al., 2018).
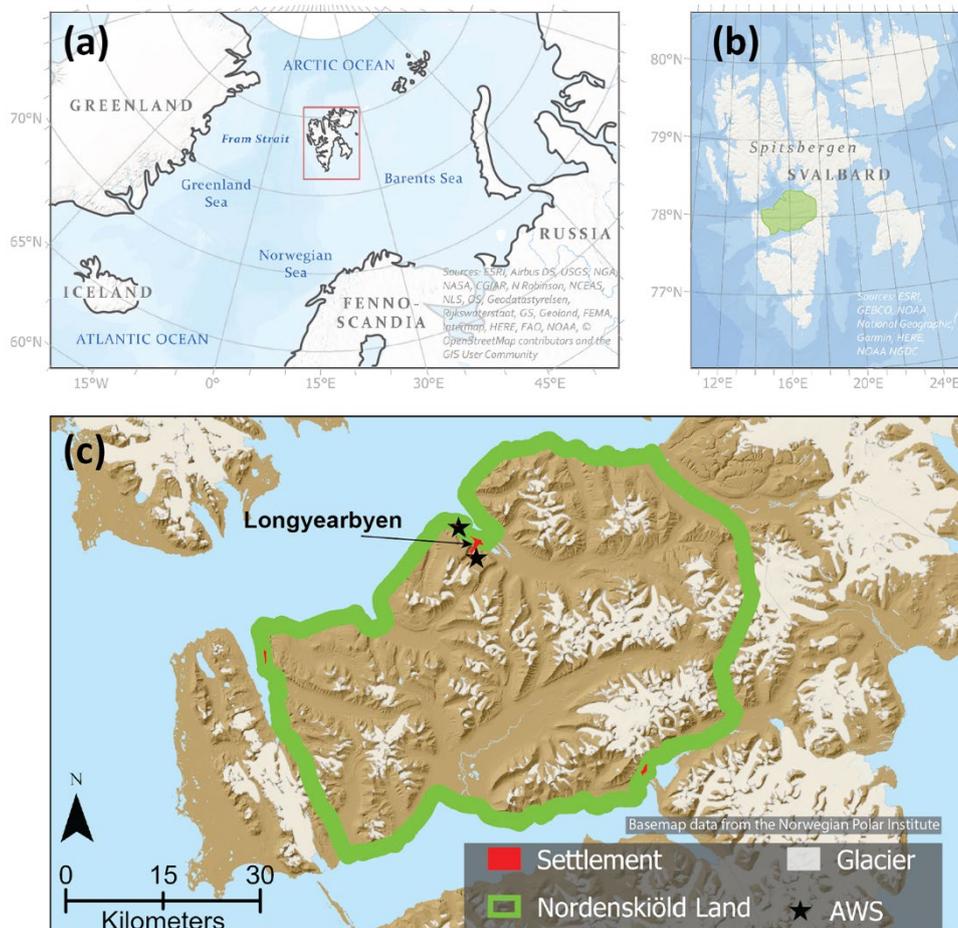
Figure 1: Panel (a) displays Svalbard's location (extent of panel (b) is shown by the red box) in the North Atlantic. Panel (b) presents an overview of Svalbard with the Nordenskiöld Land region, detailed in panel (c), highlighted in green. © OpenStreetMap contributors 2020. Distributed under a Creative Commons BY-SA License.

100 Dramatic recent changes have been superimposed on the region's baseline climatic variability, however, and likely portend similarly shifting norms in the snow avalanche climate. Air temperatures over Svalbard have increased on the order of 3-5°C between 1971 and 2017, with warming particularly pronounced during the winter months (Hanssen-Bauer et al., 2019). Trends in precipitation are generally increasing but less clearly (e.g. Førland et al., 2020; Hanssen-Bauer et al., 2019), and increased extreme precipitation event frequency has been observed in recent decades (Dobler et al., 2019; Serreze et al., 2015). These

105 changes have implications for Nordenskiöld Land's snow climate, with observed and projected increases in winter temperatures (Hanssen-Bauer et al., 2019) and rain-on-snow (ROS) event frequency (Peeters et al., 2019; Vikhamar-Schuler et al., 2016; Wickström et al., 2020) combined with shorter snow seasons (e.g. López-Moreno et al., 2016) affecting winter storm characteristics, snowpack duration and composition, and – inferentially, at least – avalanche activity.

The present study builds on this growing body of climatological research to investigate the influence exerted by synoptic-scale
atmospheric circulation on avalanche activity in Nordenskiöld Land. Our specific aims are to:

- Construct a record of recent avalanche activity using crowd-sourced avalanche observation data from the Norwegian Water Resources and Energy Directorate's (NVE) online snow and avalanche observation registration portal (www.regobs.no);

- Investigate the synoptic controls on avalanche activity in Nordenskiöld Land with reference to a well-established subjective atmospheric circulation classification for the Svalbard region;

- Place the observed synoptic controls on regional avalanche activity within the larger context of environmental change in the high Arctic.

2 Data and Methods

2.1 Avalanche observations and avalanche activity index calculations

A four-winter-season (2016/2017 – 2019/2020) record of avalanche activity for the Nordenskiöld Land region of central Spitsbergen comprises the primary dataset unique to this work. We used snow and avalanche observations stored in the regObs (an abbreviation for registration of observations) registry and made publicly – and freely – available by the Norwegian Water Resources and Energy Directorate (NVE) at https://www.regobs.no/. RegObs is NVE's system for acquiring both crowd-sourced and professional observations for natural hazard forecasting purposes in Norway and consists of a mobile app, a website, and a database accessed via an application programming interface (API) (Engeset et al., 2018). Users upload an observation via an interface on either the mobile app or the website which is then immediately displayed and stored for others to view and/or access later via the API. We focus on the snow and avalanche observations registered in regObs for the Nordenskiöld Land region of central Svalbard. These observations form the basis for public avalanche advisories issued by the Norwegian Avalanche Warning Service (NAWS) for Nordenskïold Land, the only portion of Svalbard for which public avalanche bulletins are regularly issued due to the concentration of human activity near Longyearbyen (Fig. 1). Observation quantity and quality became reliable in Nordenskiöld Land for the 2016/2017 winter season coincident with the initiation of public avalanche forecasts issued by the NAWS and the hiring of trained observers to provide regular snow and avalanche observations via regObs. We accordingly chose this winter season to begin our avalanche activity analyses, with the winter season in this work defined as December 1 – May 31 and corresponding to the period for which daily avalanche advisories are issued.
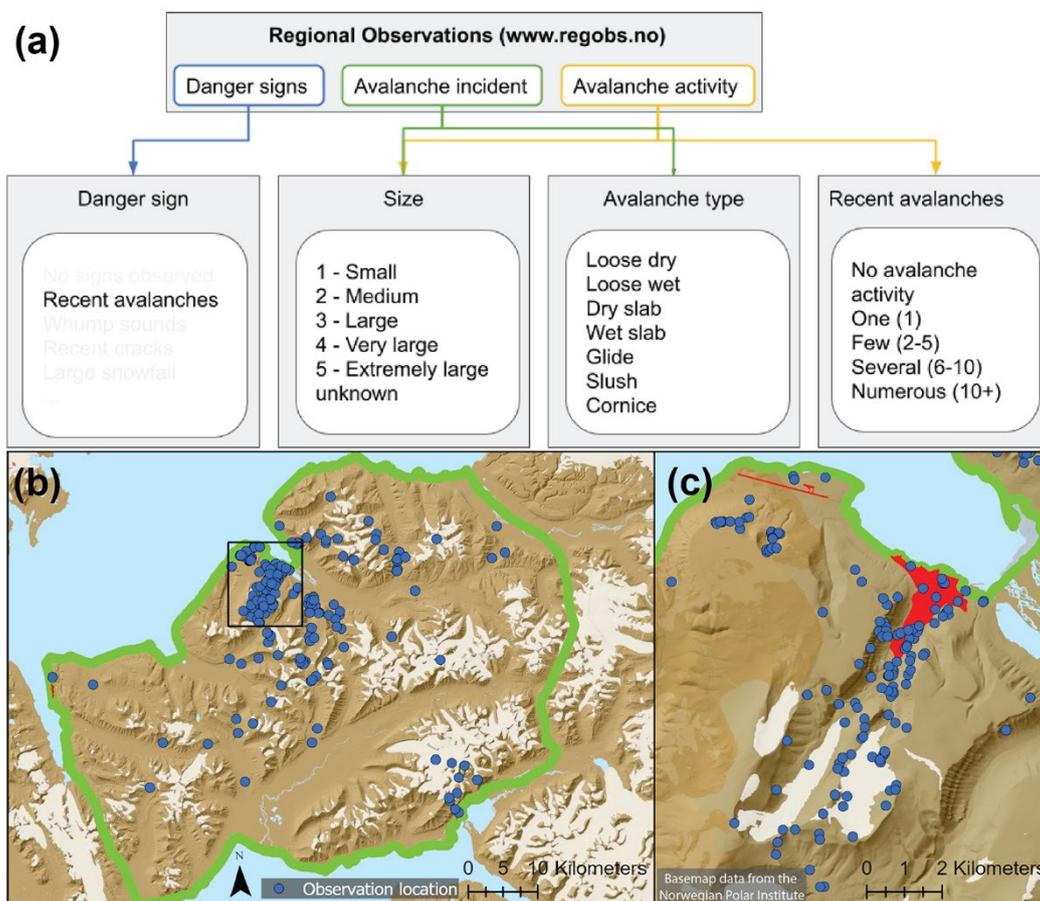
Figure 2: Overview of the regObs observations employed in this work. Panel (a) shows a schematic dispaling the regObs observation types retrieved in this work, the parameters we analyzed from each observation type, and the values for each parameter available for user selections. Note *avalanche accidents* are not displayed in this figure as they have the same parameters as avalanche incidents and, as of June 2020, are only available for input on the website and not the mobile application. Panel (b) shows the distribution of observations reporting avalanche activity used in this work, while panel (c) highlights observation density near Longyearbyen in the region indicated in panel (b).

We considered regObs observations classified as *avalanche activity*, *avalanche incidents*, *avalanche accidents*, and *danger signs* and located within the Nordenskiöld Land forecasting area when constructing our avalanche records (Fig. 2). *Avalanche activity* observations can report multiple avalanches of similar avalanche types and size for a specified timeframe, single avalanches, or no observed avalanches ("no avalanche activity observed"). These observations typically include a specification of avalanche type and destructive size, a categorical estimate of the number of observed avalanches (0, 1, 2-5, 6-10, >10), and, ideally, a photo. *Avalanche incident* observations report single avalanche occurrences and are often used for detailed descriptions of single avalanche events. *Avalanche accidents* are reported similarly to avalanche incidents, but typically involve human activity either through triggering or impact of the avalanche (i.e. danger to infrastructure). Recent avalanches can also be recorded as a *danger sign* observation.

We used the API implemented in Python made available by NVE (Ekker, 2019; last access 2020-06-06) to retrieve all avalanche activity, avalanche incident, and avalanche accident observations in addition to records where recent avalanches were listed as a danger sign from the regObs database for the Nordenskiöld Land forecasting region to create our avalanche
155   activity record. From the API's output including the registration ID, we manually checked all 678 observations on the regobs.no website to identify individual avalanches. Of these 678 observations, 385 reported avalanches while 293 were avalanche activity observations with "no avalanches observed." Manual checks allowed us to discard avalanches registered on multiple occasions or resulting from unreliable observations, correct egregious errors in observed avalanche sizes via visual checks of avalanche photos, and precisely identify the number of individual avalanches included in avalanche activity observations. For
160   the latter, we identified individual avalanches either through visual inspection of photos included with the observation or via the text description of the avalanche activity where individual avalanches may have been mentioned. In situations where neither photos nor the text sufficed to identify individual avalanches, we conservatively estimated the number of avalanches based on the lower limits of the number category such that an observation recording Several (6-10) size 1 avalanches would be recorded as six individual size 1 avalanches. We discarded 110 of the 385 (31%) records of all observation types reporting avalanches
165   in which the observed avalanches were duplicated in other observations or we could not determine an avalanche date, size, type, or number either via the avalanche parameters listed by the user or via our own inspection of the observation online. Our final database included 632 individual avalanches recorded in 275 separate avalanche observations (Fig. 2). Avalanches are primarily observed on the date they occur, but in some cases the observer has changed the date based on their knowledge of the avalanche situation or we have changed the date based on our records or the information included in the observation.

170   Using this daily record of avalanche activity, we calculated a daily avalanche activity index based on the number of observed avalanches and their estimated destructive size, using the formula from, and weighing the size classes after, Schweizer et al. (2003b). Similar to Schweizer et al. (2020), we weighed natural avalanches as 1 and human-triggered avalanches as 0.5, with avalanches with an unknown or unspecified triggered assumed to be natural and thus assigned a weight of 1. We further sub-classified wet and dry AAI components such that dry avalanches contributed to the daily Dry AAI and wet avalanches
175   contributed to the daily Wet AAI which were then summed to produce the daily AAI. We considered days with only a Dry AAI as a "Dry" avalanche type day, days with only a Wet AAI as "Wet", and days with both dry and wet AAI contributions as "Mixed." We classified 34 days with an AAI greater than or equal to 0.4 as "avalanche cycles", while we classified the 132 days with an AAI greater than 0 but less than 0.4 as "avalanche days" for a total of 166 days with observed avalanche activity (Fig. 3). Based on a visual inspection of the daily AAI distribution (Fig. 3), we explored AAI values of both 0.4 and 0.5 as
180   potential thresholds for this differentiation between avalanche days and avalanche cycles. We ultimately selected 0.4 as the threshold after detailed analyses indicated the difference in threshold value on the final results was relatively minor but lowering the threshold to 0.4 increased the number of avalanche cycles in our analyses which aided in, for example, more robust composite analyses.
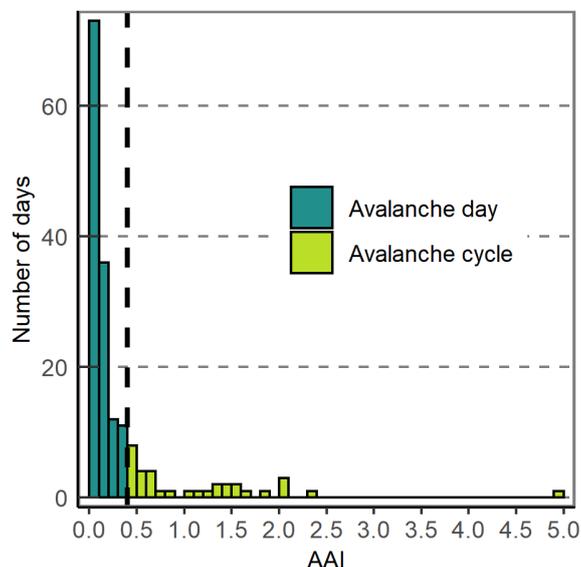
Figure 3: Distribution of the calculated daily AAI index for days where AAI > 0. The dashed black vertical line illustrates the 0.4 AAI threshold above which days were classified as avalanche cycles (n=34) and below which days were classified as avalanche days (n=132).

2.2 Atmospheric circulation

We employ a calendar of synoptic types known as the Niedźwiedź Classification (Niedźwiedź, 2013) to characterize atmospheric circulations patterns in the Svalbard region. The Niedźwiedź Classification applies methodolgy similar to Lamb's (1972) classification for the British Isles to manually define common synoptic situations over Svalbard. The Niedźwiedź Classification assesses the mean sea level pressure (MSLP) field to define common synoptic situations based on the geostrophic wind direction over Svalbard (Niedźwiedź, 2013; Isaksen et al., 2016). We use a version of the Niedźwiedź Classification synoptic types denoted by the approximate geostrophic wind direction (N+NE, E+SE, S+SW, W+NW) and if the situation is dominantly cyclonic (c) or anti-cyclonic (a). A situation with northeasterly geostrophic airflow driven by low-pressure, cyclonic activity would be thus be denoted as N+NEc. Additional cyclonic situations denoted as Cc+Bc indicate a closed low-pressure centered (Cc) near Svalbard or a low-pressure trough in the vicinity (Bc), while anti-cyclonic situations with a high-pressure center (Ca) or a ridge (Ka) near Svalbard are denoted as Ca+Ka. Finally, situations where the synoptic situation cannot be explicitly determined are assigned an undefined type (x) such that every day since 1950 is assigned to one of these 11 synoptic types.

We use MSLP, air temperature (2 m), precipitation, and wind speed data from the ERA5 Reanalysis dataset available at 31 km horizontal resolution (Hersbach et al., 2020) to analyze meteorological conditions associated with these atmospheric circulation patterns. In combination with the Niedźwiedź Classification types, the 1-hour ERA5 reanalysis data aggregated to daily mean values (MSLP, temperature, wind speed) and accumulated daily values (precipitation) form the basis for our atmospheric

205 circulation pattern analyses. We apply composite analysis on the MSLP, air temperature, precipitation, and wind speed fields
to study the atmospheric conditions associated with each synoptic type based on the ERA5 data (Appendix A). Finally, we use
data from two automated weather stations (AWSs), the Svalbard Airport AWS (28 m elevation, 4 km west of Longyearbyen)
and the Gruvefjellet AWS (464 m, 2 km southeast of Longyearbyen) to characterize the same parameters in terms of locally-
observed meteorological conditions (Fig. 1).

210 **2.2.1 Statistical significance**

We employed Monte Carlo simulations to evaluate the statistical significance of the anomalies between the mean winter
conditions and various composites presented in our results. We considered mean winter conditions to be the overall mean for
each parameter taken across all 729 winter (December-May) days between 1 December 2016 and 31 May 2020 (Appendix B).
The Monte Carlo simulation process involved selecting a random sample of days the same length as the composite of interest

215 from all 729 winter days and repeating this process 1000 times to generate a synthetic probability distribution after Wickström
et al. (2019). In an approach similar to Hendrikx et al., (2009), we determined anomalies to be statistically significant if they
fell either below the 5th percentile for negative anomalies or above the 95th percentile for positive anomalies.

We tested significance in the differing distributions of the locally measured meteorological parameters using pairwise
Wilcoxon rank sum test with a holm p-value adjustment method. We considered distributions to be significantly different for

220 p-values less than 0.05.

3 Results

3.1 Avalanche activity

We identified 632 individual avalanches from the regObs observations. Observed avalanches are primarily destructive size 1
and 2 and naturally released (Fig. 4), with no size 4 or 5 avalanches included in our database. Avalanches were observed on

225 166 of the 729 days included in our four-season record (2016/2017-2019/2020), with 34 of these 166 days further classified as
"avalanche cycles" (with an AAI > 0.4) (Table 1). Just under half (48%) of all observed avalanches and 63% of observed size
D2 and D3 avalanches occurred on avalanche cycle days. Dry avalanches comprise a majority of observed avalanche activity
(75% of all avalanches), with wet activity dominating only the Loose and Slush – wet by definition – avalanche types. Dry
slab avalanches are the most observed avalanche type, while only one slushflow (size 3) was observed. Avalanche cycle days

230   are primarily dry (27), with mixed (4) and wet (3) avalanche cycle days comprising just 20% of all avalanche cycles.
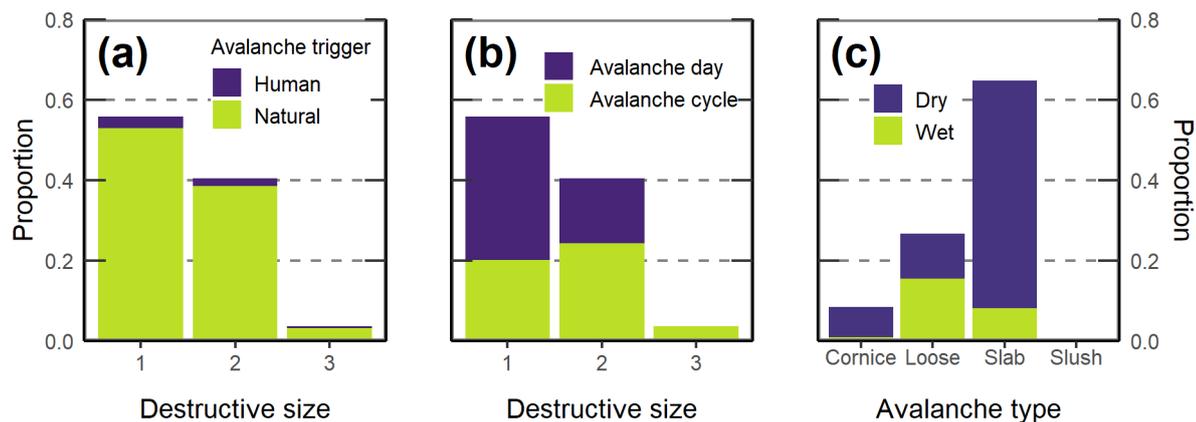
Figure 4: Summary of individual avalanches in the regObs data. Panel (a) shows the proportion of observed avalanches triggered naturally and artificially by destructive size, panel (b) shows the proportion of observed avalanches falling into major avalanche days (AAI > 0.4) by destructive size class, and panel (c) shows the proportion of observed avalanche wetness by avalanche type.

235   Days without observed avalanches in Nordenskiöld Land are typified at the synoptic scale by low pressure limited to the study
domain's southern portions (over northern Fennoscandia), with Svalbard experiencing climatological MSLP conditions (Fig.
5). This indicates the region is situated in the colder, Arctic air mass with the storm track to the south. Weakly negative
temperature anomalies over Svalbard extend southwards to Fennoscandia, with negative precipitation and wind speed
anomalies focused more directly over Svalbard and the surrounding ocean. While Svalbard is still under mean winter MSLP

240   conditions on avalanche days, high pressure anomalies dominate the southern study domain. Avalanche days are further
characterized by a narrow swath of positive precipitation anomalies extending southwards from Svalbard to the mainland, with
localized positive precipitation and wind anomalies concentrated near Spitsbergen's western coast (Fig. 5). The MLSP field
during avalanche cycles is dominated by anomalous low pressure extending from Svalbard to the northeast across the Fram
Strait. This circulation pattern is associated with stronger and more widespread positive air temperature, precipitation, and

245   wind speed anomalies over Spitsbergen relative to avalanche days (Fig. 5).
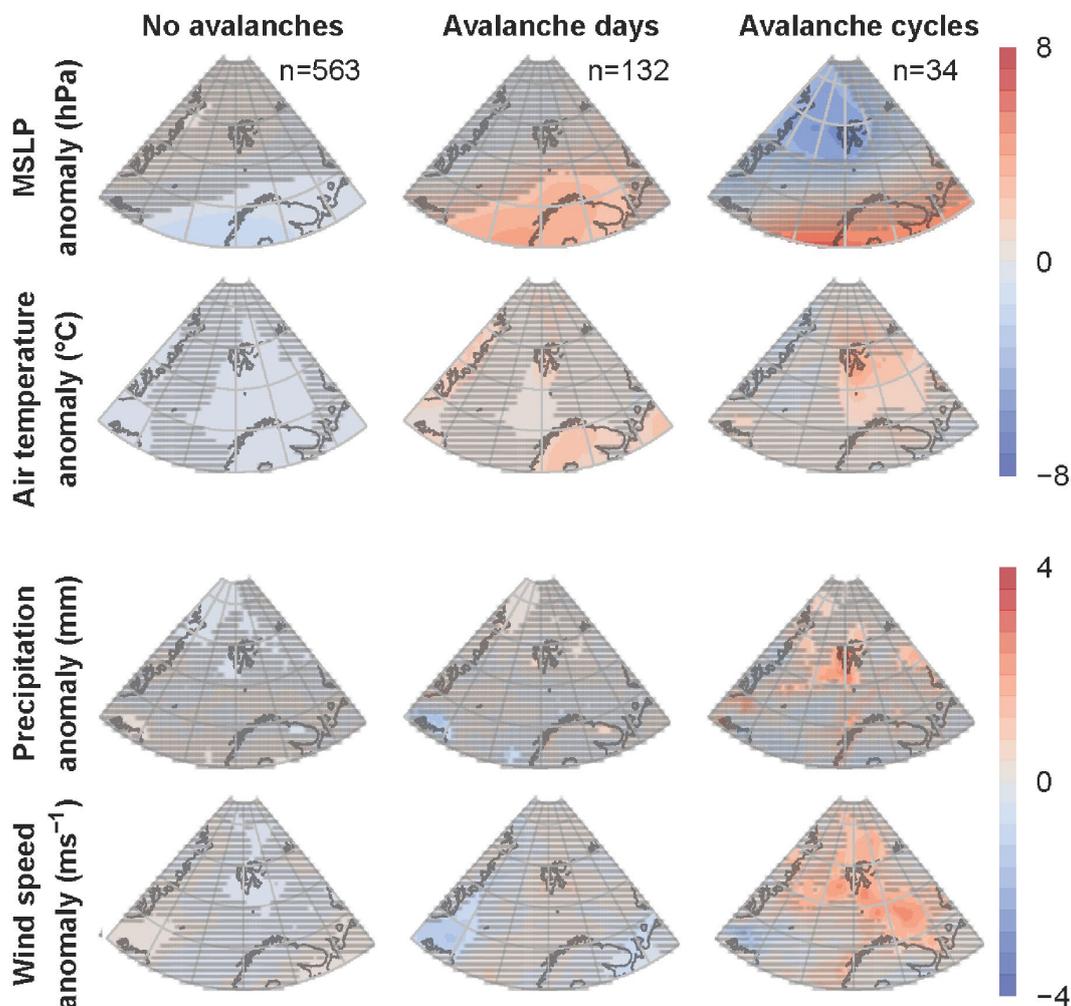
Figure 5: Composite anomaly maps for the meteorological parameters investigated in this study by the avalanche day type classification. Anomalies represent the departure from mean winter conditions (December – May, 2016-2020 – see Appendix 1) for the composite mean from avalanche day type / parameter combination. Anomalies which are not statistically significant from mean winter conditions are indicated with dense hatching.

Differences in meteorological parameters between different type of days are broadly reflected in conditions measured locally near Longyearbyen (Fig. 6). Daily air temperatures at the Gruvefjellet AWS are higher on avalanche days and avalanche cycles than on days without observed avalanches, but no statistical difference exists between air temperatures on avalanche days and avalanche cycles. Precipitation at the Svalbard Airport AWS is greater on avalanche cycle days than on avalanche days and non-avalanche days but does not statistically differ between avalanche days and non-avalanche days. Finally, daily averaged wind speeds at the Gruvefjellet AWS are significantly greater on avalanche days than on non-avalanche days and greater still on avalanche cycle days.
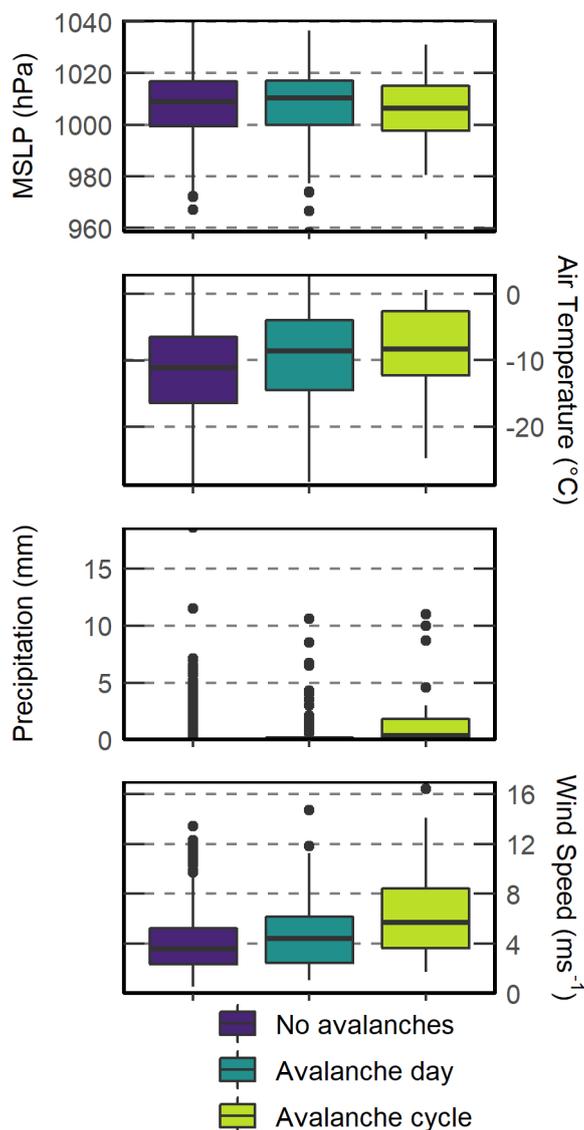
Figure 6: Boxplots showing the distributions for locally measured meteorological parameters by avalanche day type. Air temperature and wind speed are observed at the Gruvefjellet AWS, while precipitation and MSLP are observed at the Svalbard Airport AWS.

The MSLP fields differ markedly between avalanche days and avalanche cycles characterized by dry, mixed, and wet avalanche activity (Fig. 7). Dry avalanche days do not significantly differ from mean MSLP conditions near Svalbard, while significant low-pressure anomalies are centered over Svalbard during dry avalanche cycles. These circulation patterns are reflected in other meteorological parameters, with dry avalanche days only significantly differing from mean conditions with a limited area of slightly positive wind speed anomalies southeast of Svalbard (Fig. C3). Dry avalanche cycles show widespread significantly positive precipitation and wind speed anomalies in conjunction with the low-pressure anomaly over the region

(Fig. C2 and Fig C3). On wet avalanche days, by contrast, Svalbard is encompassed by strongly positive MLSP anomalies stretching from Fennoscandia across the Barents Sea. This pattern is more pronounced during wet avalanche cycles, although

270   the region over which the positive anomalies are significant decreases likely due to the limited sample size (Fig. 7). Both wet avalanche days and cycles exhibit strongly positive air temperature anomalies over Svalbard (Fig. C1), wet avalanche cycles show a thin strip of significant positive precipitation anomalies extending southwest from central Spitsbergen (Fig. C2), and wind speeds do not significantly differ from mean winter conditions on either wet avalanche days or cycles (Fig. C3). MSLP patterns on avalanche days and avalanche cycles with mixed avalanche activity closely resemble those associated with wet

275   activity, but the high-pressure ridge over Fennoscandia is somewhat flattened just south of Svalbard and does not extend as dramatically northwards into the Barents Sea (Fig. 7). Mixed avalanche days and cycles also show significant positive temperature anomalies (Fig. C1), but other significant anomalies are restricted to a very limited positive precipitation anomaly region in northwestern Spitsbergen and a region of positive wind speed anomalies southeast of the island during mixed avalanche cycles.

280
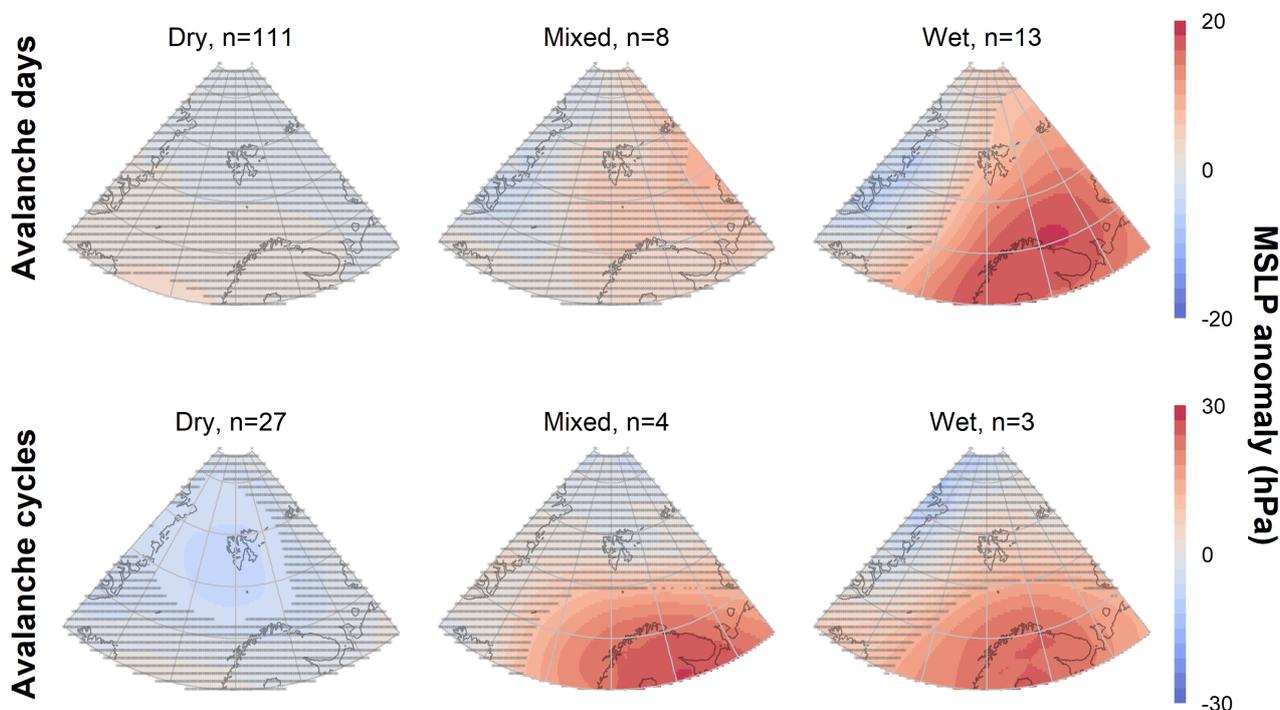
Figure 7: Maps of composite MSLP anomalies versus mean winter MSLP conditions (Dec-May, 2016-2020) by dry, mixed, and wet avalanche activity classifications. Anomalies which are not statistically significantly different from mean winter conditions are indicated with dense hatching. Additional parameter plots are found in Appendix C.

285 At the AWSs near Longyearbyen, higher air temperatures are observed on mixed and wet avalanche days and avalanche cycles than on dry avalanche days and avalanche cycles (Fig. 8). Wind speeds and daily accumulated precipitation, however, do not statistically differ between dry, mixed, and wet avalanche days and avalanche cycles.
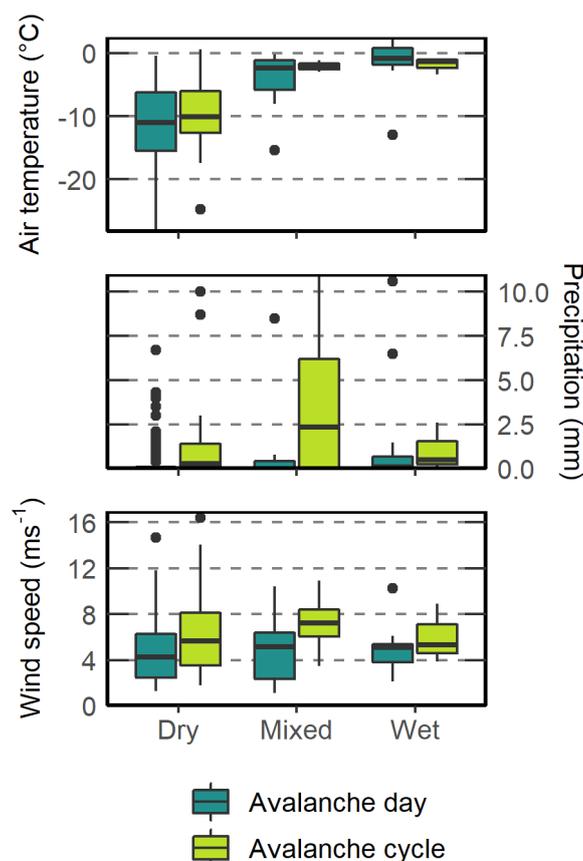
Figure 8: Boxplots showing the distributions for locally measured meteorological parameters by dry, mixed, and wet avalanche
290 **activity classifications. Air temperature and wind speed are observed at the Gruvefjellet AWS, while precipitation is observed at the Svalbard Airport AWS.**

3.2 Connection with established synoptic classifications

We characterize 729 winter days by synoptic type and avalanche activity (Table 1). The most common synoptic types are Types 6 (N+NEc), 7 (E+NEc), and 10 (Cc+Bc). The least frequently observed synoptic types are Types 4 (W+NWa), 9
295 (W+NWc), and 3 (S+SWa). The synoptic types with the highest proportion avalanche days with observed avalanche activity are Types 9 (W+NWc), 4 (W+NWa), and 8 (S+SWc), while Types 9 (W+NWc), 4 (W+NWa), and 10 (Cc+Bc) have the highest proportion of avalanche cycle days. Synoptic types dominated by cyclonic airflow –Types 6 (N+NEc), 7 (E+Sec), 8 (S+SWc), 9 (W+NWc), and 10 (Cc+Bc) – contain most avalanches and comprise most avalanche cycle days, while occurring on over 70% of winter days (Fig. 9, Table 1). Synoptic types dominated by anti-cyclonic airflow – Types 1 (N+NEa), 2

(E+SEa), 3 (S+SWa), 4 (W+NWa), and 5 (Ca +Ka) – occur less frequently (on roughly 30% of winter days) and in some cases do not contain a single avalanche cycle (Types 2 (E+NEa) and 5 (Ca+Ka)). Dry avalanches dominate observed avalanche activity for all synoptic types except Types 3 (S+SWa) and 9 (W+NWc), during which wet avalanches are more frequently observed (Fig. 9). Similarly, avalanche cycles are dominated by dry activity, with the exceptions of Types 3 (S+SWa), 9 (W+NWc), 10 (Cc+Bc), and 11 (x – unclassified) which all include avalanche cycles with mixed or wet activity. The most common winter synoptic types – Types 6 (N+NEc), 7 (E+Sec), and 10 (Cc+Bc) – also contain the greatest absolute number of avalanche cycles, while a relatively uncommon synoptic type – Type 9 (W+NWc) – has by far the highest proportion of days classified as avalanche cycles (Table 1). Case studies selected for illustrative purposes representative of these two situations are further investigated in the following sub-sections.

Table 1. Distribution of total winter days, avalanche days, and avalanche cycles by AC type after Niedźwiedź (2013). Maximum values for each column are displayed in **bold.** Appendix A shows the composite parameter field anomalies for each synoptic type over our period of record.

Synoptic type (numeric identifier)	Synoptic type (airflow descriptor)	Total number of winter days	# of avalanche days	# of avalanche cycles	Proportion of winter days classified as synoptic type	Proportion of days classified as avalanche days	Proportion of days classified as avalanche cycles
1	N+NEa	73	14	2	0.10	0.19	0.03
2	E+SEa	48	9	0	0.07	0.19	0
3	S+SWa	26	3	2	0.04	0.12	0.08
4	W+NWa	11	4	1	0.02	0.36	0.09
5	Ca+Ka	69	8	0	0.09	0.12	0
6	N+NEc	**174**	**25**	6	**0.24**	0.14	0.03
7	E+Sec	120	18	5	0.16	0.15	0.04
8	S+SWc	59	22	3	0.08	0.37	0.05
9	W+NWc	17	7	4	0.02	**0.41**	**0.24**
10	Cc+Bc	89	11	**8**	0.12	0.12	0.09
11	x	43	11	3	0.06	0.26	0.07
Total		729	132	34	NA	0.18	0.05
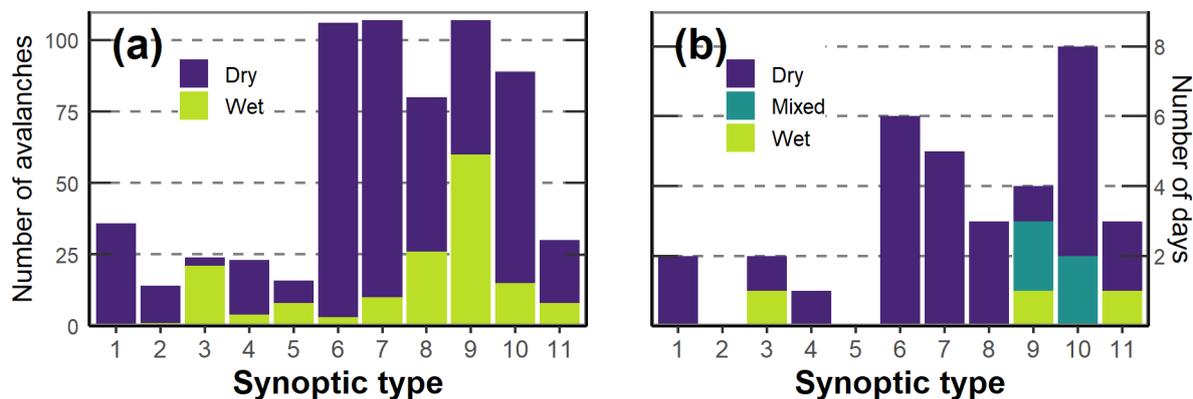
Figure 9. Avalanche activity by synoptic type denoted by the numeric identifier. Panel (a) shows the total number of wet and dry avalanches observed during days of each synoptic type, and panel (b) displays the number of major avalanche cycles classified by avalanche activity wetness for each synoptic type.

3.2.1 Type 9 (W+NWc): An infrequent synoptic type with frequent avalanche cycles

Avalanche cycles occur on nearly one in four days on Type 9 (W+NWc) days, and well over half of all Type 9 (W+NWc) days are classified as either avalanche cycles or avalanche days (Table 1). Relative to other synoptic types, however, Type 9 (W+NWc) conditions occur infrequently; only Type 4 (W+NWa) – characterized by anti-cyclonic from the same direction as Type 9 (W+NWc) – occurs less frequently. Type 9 (W+NWc) conditions are associated with a low pressure situated northeast of Svalbard and a ridge of high pressure over Fennoscandia, promoting west-northwesterly airflow from across the ice-free Fram Strait over central Spitsbergen. Relative to mean winter conditions, Type 9 (W+NWc) days are characterized by a thin band of positive precipitation anomalies concentrated along Spitsbergen's western coast in addition to the more widespread positive anomalies located north and northeast of Svalbard (Fig. 10). Air temperatures are warmer than mean winter conditions across most of the domain, with an isolated area of negative temperature anomalies located just west of Spitsbergen in the Fram Strait. Wind speeds are increased relative to mean winter conditions over the Norwegian Sea to the south of Spitsbergen.

Synoptic conditions during Type 9 (W+NWc) avalanche cycles do not differ significantly from the mean Type 9 (W+NWc) state (Fig. 10). Although the composite avalanche cycle MSLP field shows slight deepening of the low to the northeast of Svalbard relative to the mean MSLP field, this deepening is not statistically significant (Fig. 10). Similarly, lightly positive precipitation and air temperature anomalies over central Spitsbergen for Type 9 (W+NWc) avalanche cycles are not statistically significant relative to mean Type 9 (W+NWc) conditions. Wind speeds over Svalbard differ very little from the Type 9 (W+NWc) mean state, with statistically significant wind speed anomalies concentrated to the southeast of the archipelago. Strongly positive temperature anomalies resulting from this synoptic type place Nordenskiöld Land in warm air hovering near freezing, where variability in air mass characteristics can result in dry, mixed, or wet avalanche cycles (the only synoptic type

to encompass all three avalanche cycle types). These conditions resulting from Type 9 (W+NWc) airflow with a low pressure
northeast of Svalbard occur infrequently, but they often produce avalanche cycles when they do occur, and the synoptic

335 environment does not need to significantly differ from the Type 9 (W+NWc) mean state to result in avalanche cycles.
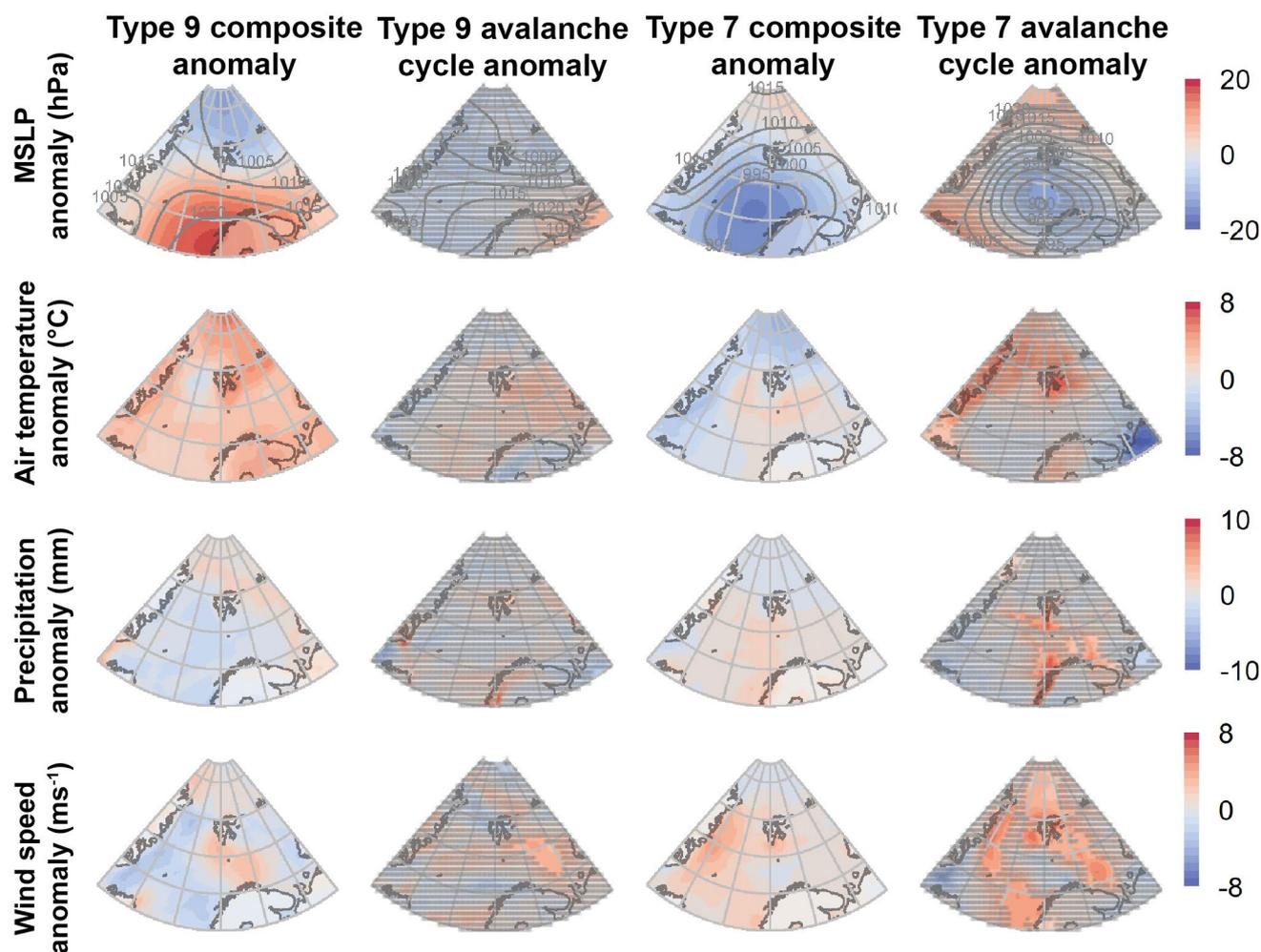
**Figure 10: Composite anomalies for all Type 9 and Type 7 winter days vs mean winter conditions and anomalies for Type 9 and
Type 7 avalanche cycles vs Type 9 and Type 7 composites, respectively. Avalanche cycle anomalies which are not statistically**
340 **significantly different from the respective synoptic type's composite are indicated with dense hatching.**

3.2.2 Type 7 (E+SEc): A common synoptic type with infrequent avalanche cycles

Type 7 (E+SEc) conditions, in contrast to Type 9 (W+NWc) situations, are common throughout the winter months, but do not frequently produce avalanche cycles on a relative basis. These conditions occur when a low-pressure center situated generally

345 southeast of Svalbard promotes easterly-southeasterly airflow over central Spitsbergen (Fig. 10). This situation is common during the winter months due to high cyclone density and an active storm track in the Norwegian Sea, with only Type 6 (N+NEc) conditions occurring more frequently during the observational period. The low pressure's location during mean Type 7 (E+Sec) conditions promotes lightly positive precipitation and air temperature anomalies in the Norwegian Sea and the Fram Strait relative to overall mean winter conditions (Fig. 10). Wind speeds stronger than mean winter conditions are concentrated

350 near Spitsbergen's southern tip. During avalanche cycles representing approximately just 4% of all Type 7 (E+SEc) days, the low-pressure center significantly deepens and shifts to the northeast (Fig. 10) – the only synoptic type to show widespread significant departures from its mean MSLP state during avalanche cycles. This results in significantly wetter, warmer, and windier conditions over Spitsbergen than the mean Type 7 (E+SEc) state (Fig. 10). All Type 7 (E+SEc) avalanche cycles are dry despite the positive temperature anomalies. The significant differences between the Type 7 (E+SEc) mean state and the

355 conditions resulting in Type 7 (E+SEc) avalanche cycles show the anomalously deep low pressure center south of Spitsbergen promotes the synoptic environment required to produce avalanche cycles under this synoptic type. Thus, while Type 7 (E+SEc) days encompass a large absolute number of avalanche cycles, avalanche cycles conditions represent infrequent, but significant departures from the mean Type 7 (E+SEc) state.

4 Discussion

360 ### 4.1 Synoptic controls on avalanche activity

Our results indicate atmospheric circulation patterns leading to wet, windy, and warm conditions over Nordenskiöld Land are associated with increased observed regional avalanche activity. The conditions are commonly related to cyclonic airflow related to low-pressure systems transported northwards along the North Atlantic storm track. In aggregate, avalanche cycle days display a clear low-pressure signal, with cyclonic activity in the Fram Strait drawing in the warm, wet air represented by

365 the positive air temperature and precipitation anomalies (Fig. 5). These controls are further demonstrated by the inverse situation where days without observed avalanche activity show decreased wind speeds, precipitation, and air temperatures over Svalbard relative to mean winter conditions. Cyclonic control is also broadly evident when considering avalanche activity by synoptic type, as synoptic types driven by cyclonic airflow dominate both in terms of total observed avalanches (Fig. 9a) and in the number of avalanche cycles (Fig. 9b). Furthermore, the specific synoptic circulation type characterized by a low-pressure

370 center or trough directly over Svalbard – Type 10 (Cc+Bc) – results in the most avalanche cycle days. The Type 5 (Ca+Ka) synoptic type – high pressure over Svalbard characterizing a drier, calmer synoptic environment – by contrast did not result in a single avalanche cycle. These results largely confirm previous characterizations of Nordenskiöld Land's direct-action

avalanche regime where snowfall, increased wind speeds, and increased air temperatures related to winter storms are precursors to widespread avalanche activity (Eckerstorfer and Christiansen, 2011b, 2011c; Hancock et al., 2018).

375 While atmospheric circulation conducive to increased precipitation, wind speeds, and air temperatures in the vicinity of Svalbard generally control avalanche timing here, airflow direction considerably influences the nature of observed avalanche activity. We found observed wet avalanche activity to be primarily associated with airflow from the southerly through northwesterly airflow synoptic types (e.g. Types 3 (S+SWa), 4 (W+NWa), 8 (S+SWc), and 9 (W+NWc)), while dry activity dominates northerly and easterly airflows (e.g. Types 1 (N+NEa), 6 (N+NEc), and 7 (E+SEc)). These findings align well with
380 previous work employing the Niedźwiedź (2013) classification showing synoptic types resulting in southerly and westerly airflow over Spitsbergen result in higher temperatures and are most frequently associated with precipitation at the Svalbard Airport AWS (Isaksen et al., 2016; Wickström et al., 2020). Synoptic types with an easterly or northerly airflow component were found to be colder and drier than their southerly and westerly counterparts (Førland et al., 2020; Wickström et al., 2020).

The Type 7 (E+SEc) and Type 9 (W+NWc) synoptic type case studies further reflect these synoptic controls. The significant
385 low-pressure anomaly due south of Spitsbergen during Type 7 (E+SEc) avalanche cycles relative to Type 7 (E+SEc) mean conditions promotes strong and wet enough easterly airflow to convey precipitation across eastern Spitsbergen's orographic barrier to Nordenskiöld Land. Sea ice limits upwind sea to air heat exchange in this scenario, and the low-pressure's positioning places Spitsbergen in the colder, Arctic airmass with the jet stream to the south. Precipitation thus falls as snow during Type 7 (E+SEc) avalanche cycles despite positive temperature anomalies relative to mean Type 7 (E+SEc) conditions, and avalanche
390 activity is dry.

By contrast, low pressure to the northeast of Svalbard and high pressure to the south typifies Type 9 (W+NWc) conditions and results in westerly airflow across Nordenskiöld Land. Upwind conditions in this synoptic environment differ considerably from Type 7 (E+SEc) conditions, with warm Atlantic water off Spitsbergen's west coast serving as a heat and moisture source for the westerly, onshore airflow. Nordenskiöld Land is situated on Spitsbergen's windward portion in this scenario, and
395 precipitation is orographically enhanced. Westerly is particularly conducive to avalanche activity, as further evidenced by the high proportion of avalanche days and avalanche cycles from Type 4 (W+NWa) circulation, despite the overall anti-cyclonic dominance of this synoptic type (Table 1). Type 9 (W+NWc) mean state conditions are therefore more readily conducive to supplying the ingredients for avalanches than mean Type 7 (E+SEc) conditions, as Type 9 (W+NWc) avalanche cycle synoptics do not appear to differ significantly from the Type 9 (W+NWc) mean state. The prevalent wet component observed
400 in Type 9 (W+NWc) avalanche activity – suggesting positive air temperatures and liquid precipitation falling in Nordenskiöld Land – reflects the heat available to the airmass from the upwind open ocean. One Type 9 (W+NWc) avalanche cycle contained only dry avalanches, however, indicating this synoptic situation is not necessarily diagnostic of wet avalanche activity.

The composite MSLP fields for dry, mixed, and wet avalanche activity days and cycles (Fig. 7) further reinforce the synoptic controls on avalanching in Nordenskiöld Land. Statistically significant low-pressure anomalies in Svalbard's vicinity

405   characterize the MSLP fields for dry avalanche cycles, while high pressure over Fennoscandia and the Barents Sea dominates during mixed and wet cycles. Low pressure near Svalbard during dry avalanche cycles emphasizes again the clear cyclonic control on dry avalanche activity in Nordenskiöld Land and represents the most frequently observed synoptic situation leading to avalanches here, providing the snow available for transport and wind speeds necessary to develop dry avalanche conditions. Less frequently, strongly positive MSLP anomalies in the study domain's southern portion lead to mixed and wet avalanche

410   days and cycles. This finding suggests the Scandinavian blocking pattern, where high pressure over Fennoscandia directs warm, wet air masses to Svalbard, leads to wet avalanches in Nordenskiöld Land. These results encouragingly align with other work which has linked similar synoptic patterns characterized by south-southwesterly airflow over Svalbard with extreme precipitation events in western Spitsbergen (Serreze et al., 2015) and rain-on-snow events throughout the archipelago (Wickström et al., 2020). Such a synoptic environment allows heat and moisture from lower-latitude Atlantic source regions

415   to be efficiently transported to Svalbard, providing the warm air and liquid precipitation required to develop conditions conducive to wet avalanche release. While an association between extreme precipitation and rain-on-snow events with wet avalanche activity is intuitive, it is helpful to specifically place these linked processes within the same synoptic context.

4.2 Implications

4.2.1 Environmental change

420   Documented increases in air temperature (e.g. Isaksen et al., 2016; Nordli et al., 2020), increasing precipitation and shifting precipitation regimes (e.g. Førland et al., 2020), changing storm tracks (e.g. Wickström et al., 2019), and declining sea ice (e.g. Muckenhuber et al., 2016; Onarheim et al., 2014) have broad implications for Svalbard's physical environment. Previous research on Spitsbergen has investigated the influence of climatic changes on snowpack characteristics in the recent past (e.g. Peeters et al., 2019; van Pelt et al., 2016), but a lack of robust avalanche activity records impedes avalanche-specific analyses

425   over longer temporal scales. Projecting future changes to avalanche regimes in this and other locations is further hindered by the complex interactions between the meteorological and snowpack parameters influencing avalanche release and the difficulty resolving finer-scale snow and avalanche processes with the resolution currently available in climate models (e.g. Beniston et al., 2018). Predictions related to future avalanche activity have therefore primarily focused on broader spatial scales and changes to the overall avalanche regime, with expectations of increasing wet avalanche activity dominating projections in

430   other snow avalanche climates (e.g. Ballesteros-Cánovas et al., 2018; Castebrunet et al., 2014; Dyrrdal et al., 2020). Although we are unable to specifically investigate changes to central Spitsbergen's avalanche regime given our avalanche activity record's considerable limitations, we argue that connecting observed avalanche activity to synoptic atmospheric circulation patterns helps frame avalanche processes within the larger context of environmental change. As an example, we link wet avalanches in Nordenskiöld Land to specific synoptic conditions allowing warm air advection to central Svalbard from the

435   south and west. Isaksen et al. (2016), however, noted a correlation between decreasing wintertime sea ice north and east of Svalbard with warmer airflow from these locations, and Wickström et al. (2020) discuss how the ice-free ocean here promotes

enhanced precipitation during the early winter season with northerly airflow. With continued background warming superimposed on warmer, moister upwind conditions related to decreased sea ice in the Barents Sea, one might expect to see more frequent and prevalent wet avalanche activity with easterly airflow – airflow which currently results in primarily dry

440 avalanche activity – should air temperatures rise sufficiently. Future research can therefore build upon this work to address questions related to the changing avalanche regime in central Svalbard by, for example, disentangling the relative influence of specific atmospheric circulation patterns, changes to their associated upwind conditions, and general background warming on future wet avalanche activity in this location.

4.2.2 Hazard management

445 Avalanches present documented hazards to human life and infrastructure in Svalbard, with numerous fatalities occurring in both recreational accidents and infrastructure-related events over the past decade (Engeset et al., 2020; Hancock et al., 2018) Currently, formalized avalanche hazard assessments throughout the winter months in Svalbard include daily regional public avalanche hazard bulletins for Nordenskiöld Land issued by the NAWS and a daily local avalanche hazard bulletin for local officials issued for the infrastructure in Longyearbyen by Skred AS, a consulting firm (Engeset et al., 2020). Our results can

450 help inform avalanche forecasters and hazard managers in this setting by helping resolve avalanche processes at the synoptic-scale which, in combination with more scale-appropriate data for a specific forecasting problem (e.g. slope-scale data for a slope-specific avalanche forecast), form the basis for accurate and precise hazard forecasts (LaChapelle, 1980; McClung, 2002b). For example, we identify westerly, onshore airflow as a synoptic situation particularly conducive to avalanche activity in Nordenskiöld Land. Long range synoptic-scale weather forecasts can then be used to identify these situations well in advance

455 and refine the hazard assessment with finer spatial and temporal scale weather and snowpack data as it becomes available. Across longer temporal scales, our results showing dry avalanche cycles related to low pressure near Svalbard (Fig. 5) can be linked to other work showing these situations are occurring more frequently in the modern climate (Wickström et al., 2019) to help anticipate changing frequencies of avalanche events and plan hazard management strategies accordingly.

In locations where a subjective atmospheric circulation pattern classification such as the Niedźwiedź Classification employed

460 in this work is unavailable, objective classification techniques offer researchers and hazard managers an avenue to improve the synoptic-scale understanding of avalanche processes. Self-organizing maps, for example, have recently been used to classify atmospheric circulation patterns leading to deep slab avalanches in the western United States (Schauer et al., 2020). The synoptic types identified using such an objective approach can then be used, as in this study, to identify the synoptic controls on avalanche activity and better inform hazard management decisions.

465 ### 4.3 Study limitations

This study represents a first-order attempt at understanding the synoptic controls on snow avalanching in central Svalbard, but conclusions drawn from this work are limited by the study's restricted temporal coverage and uncertainties in our avalanche

record. Using the regObs database from 2016 onwards gave us access to the best available avalanche data for Nordenskiöld Land, but the resulting four-season record is insufficient for to be considered a true climatological study. This is especially
470   true in Svalbard, where modern conditions are not representative of conditions even a decade or two prior. Our results are thus best interpreted as a snapshot of the contemporary avalanche setting likely differing both from even recent past and near-future avalanche conditions. We also chose to use mean winter conditions derived from these four winter seasons rather than from across the entire 1979-2020 timeframe for which ERA5 data is available when calculating anomalies. Using composite anomalies calculated from selected days (e.g. non-avalanche days, avalanche days, or avalanche cycles) compared against
475   mean winter conditions from the 1979-2020 period resulted in statistically significant positive air temperature anomalies across the entire domain regardless of the selected day type. We thus elected to consider mean winter conditions as the four-season mean to better differentiate between the primary day types of interest to this work, as our research objectives focused primarily on differentiating the synoptic controls on avalanche activity rather than specifically investigating the impacts of climatic changes across a longer time series.

480   Considerable uncertainties in the avalanche activity record also limit interpretation of our results. Our avalanche activity record relies on observations from users with varying degrees of experience. This means many of the avalanche parameters used in our analyses (e.g. avalanche size, avalanche type, date of avalanche release) are derived from subjective, judgement-based observations from potentially untrained users. Furthermore, avalanche activity observations are clustered in the portion of Nordenskiöld Land immediately surrounding Longyearbyen. While unsurprising given most human activity – and,
485   consequently, avalanche exposure – occurs in this area, the observation distribution implies our results are most representative for the Longyearbyen area and may be less robust for other areas in Nordenskiöld Land. More objectively detecting avalanche activity across Nordenskiöld Land through, for example, satellite observations would help improve the robustness of our results and resulting interpretations (e.g. Bühler et al., 2019; Eckerstorfer et al., 2019). Until satellite products with sufficient temporal resolution and spatial coverage to reliably detect avalanches are available for Svalbard, however, we believe the regObs data
490   are a robust alternative for investigating regional avalanche activity.

Uncertainty related to avalanche timing has arguably the greatest potential to affect our analyses when attempting to link avalanche release to specific meteorological conditions. We have attempted to reduce uncertainties related to observation quality by manually checking each observation as described in Section 3.1 and discarding observations for which the quality is too suspect, but uncertainties likely remain. While previous work in Svalbard and the results in this work suggest a strong
495   direct-action control on avalanche activity in this location, future work could more specifically target the seasonal progression of avalanche conditions (e.g. the synoptic controls on weak layer development) and should also examine conditions in the 48 and 72 hours prior to observed avalanche activity to improve the current analyses. Finally, our analyses are limited in terms of identifying non-avalanche days. In this work "non-avalanche days" are simply days without observed avalanche activity but include both days where observers explicitly did not observe avalanches in their observation and days lacking observations.

500 Despite these limitations, this work demonstrates the importance role atmospheric circulation plays in the avalanche regime in this unique setting and provides a framework for future analysis on the impacts of climate change on avalanche occurrence.

5 Conclusion

We explored the relationship between atmospheric circulation patterns across a broad portion of the North Atlantic and Arctic regions and observed avalanches in Nordenskiöld Land to investigate the synoptic-scale meteorological controls on avalanche
505 activity in central Spitsbergen. We employed crowd-sourced avalanche occurrence data available on the regObs natural hazard database from four winter seasons (2016/2017 – 2019/2020) to identify 632 individual avalanches occurring on 166 days, 34 of which we classified as avalanche cycles. Analyzing the synoptic environment associated with various avalanche activity situations allowed us to build upon previous snow avalanche work in this location by specifically addressing controls on avalanching at a broader spatial scale.

510 Our findings generally support the existing understanding of snow avalanching in Nordenskiöld Land by showing synoptic conditions leading to increased precipitation, stronger winds, and elevated air temperatures are associated with increased avalanche activity. We identified low pressure near Svalbard resulting in positive precipitation and wind speed anomalies as the aggregate synoptic signal for dry avalanche cycles, while warm air diverted northwards by a high-pressure ridge over Fennoscandia and isolated positive precipitation anomalies near Spitsbergen's west coast characterize mixed and wet
515 avalanche cycles. Further linking our avalanche activity record and analyses with a well-established subjective classification of synoptic situations over Svalbard provided an avenue to consider avalanche activity in Svalbard within the growing body cryospheric, meteorological, and climatological research for the region. We argue upwind conditions play a key role in controlling the presence or nature of avalanche activity resulting from a particular circulation pattern, which affords future opportunities to link this work to studies of past and future atmospheric and cryospheric change in this location. Furthermore,
520 these results can help hazard managers anticipate future periods of increased avalanche activity based on synoptic-scale weather forecasts. Although limited by a short analysis period and uncertainties in the avalanche record, this work provides a foundation on which to base future studies more specifically investigating the role of Svalbard's rapidly changing climate on avalanche activity here and helps place avalanches within the broader context of environmental change in the Arctic.

Data Availability

525 The dataset containing all individual avalanches retrieved from regObs and the calculated daily AAI used in these analyses is available at http://dx.doi.org/10.17632/dv4m9bbn9y.1. RegObs data is freely available from NVE on the regobs.no website. We used the methods contained in https://github.com/ragnarekker/varsomdata to access the regObs data. ERA5 data are available through the Copernicus Climate Change Service (CS3) Climate Data Store at https://cds.climate.copernicus.eu/. Data for the Svalbard Airport AWS are available through Norwegian Meteorological Institute's online data accessibility platform

530 (www.eklima.no). Data from the Gruvefjellet AWS are freely available through the University Centre in Svalbard via www.unis.no/resources/weather-stations/. Dr. Tadeusz Niedźwiedź kindly provided us his atmospheric circulation classification calendar upon request.

Author Contributions

HH, JH, and ME developed the idea for the study. HH processed and analyzed the data with assistance from SW. HH prepared
535 the manuscript with contributions from all co-authors.

Acknowledgements

We are grateful for Dr. Tadeusz Niedźwiedź's contribution of his atmospheric circulation calendar, without which this work would not have been possible in its current form. We are also thankful for NVE's work to allow user access to the considerable wealth of information contained in the regObs database.

540 **Competing Interests**

The authors declare they have no conflict of interest.

References

Ballesteros-Cánovas, J. A., Trappmann, D., Madrigal-González, J., Eckert, N., and Stoffel, M.: Climate warming enhances snow avalanche risk in the Western Himalayas, Proceedings of the National Academy of Sciences, 115, 3410-3415, doi:10.1073/pnas.1716913115, 2018.

Bednorz, E., and Fortuniak, K.: The occurrence of coreless winters in central Spitsbergen and their synoptic conditions, Polar Research, 30, 2011.

Bednorz, E., and Kolendowicz, L.: Summer mean daily air temperature extremes in Central Spitsbergen, Theoretical and Applied Climatology, 113, 471-479, 2013.

Bednorz, E., Kaczmarek, D., and Dudlik, P.: Atmospheric conditions governing anomalies of the summer and winter cloudiness in Spitsbergen, Theoretical and Applied Climatology, 123, 1-10, doi:10.1007/s00704-014-1326-5, 2016.

Beniston, M., Farinotti, D., Stoffel, M., Andreassen, L. M., Coppola, E., Eckert, N., Fantini, A., Giacona, F., Hauck, C., Huss, M., Huwald, H., Lehning, M., López-Moreno, J. I., Magnusson, J., Marty, C., Morán-Tejéda, E., Morin, S., Naaim, M., Provenzale, A., Rabatel, A., Six, D., Stötter, J., Strasser, U., Terzago, S., and Vincent, C.: The European mountain cryosphere: a review of its current state, trends, and future challenges, The Cryosphere, 12, 759-794, doi:10.5194/tc-12-759-2018, 2018.

Birkeland, K. W., Mock, C., and Shinker, J.: Avalanche extremes and atmospheric circulation patterns, Annals of Glaciology, 32, 135-140, 2001.

Björnsson, H.: Avalanche activity in Iceland, climatic conditions, and terrain features, Journal of Glaciology, 26, 13-23, 1980.

Bühler, Y., Hafner, E. D., Zweifel, B., Zesiger, M., and Heisig, H.: Where are the avalanches? Rapid SPOT6 satellite data acquisition to map an extreme avalanche period over the Swiss Alps, The Cryosphere, 13, 3225-3238, doi:10.5194/tc-13-3225-2019, 2019.

Castebrunet, H., Eckert, N., Giraud, G., Durand, Y., and Morin, S.: Projected changes of snow conditions and avalanche activity in a warming climate: the French Alps over the 2020–2050 and 2070–2100 periods, The Cryosphere, 8, 1673-1697, doi:10.5194/tc-8-1673-2014, 2014.

Clark, M. P., Hendrikx, J., Slater, A. G., Kavetski, D., Anderson, B., Cullen, N. J., Kerr, T., Örn Hreinsson, E., and Woods, R. A.: Representing spatial variability of snow water equivalent in hydrologic and land-surface models: A review, Water Resources Research, 47, doi:https://doi.org/10.1029/2011WR010745, 2011.

Cottier, F. R., Nilsen, F., Inall, M. E., Gerland, S., Tverberg, V., and Svendsen, H.: Wintertime warming of an Arctic shelf in response to large-scale atmospheric circulation, Geophysical Research Letters, 34, L10607, doi:10.1029/2007GL029948, 2007.

Dyrrdal, A. V., Isaksen, K., Jacobsen, J. K. S., and Nilsen, I. B.: Present and future changes in winter climate indices relevant for access disruptions in Troms, northern Norway, Nat. Hazards Earth Syst. Sci., 20, 1847-1865, doi:10.5194/nhess-20-1847-2020, 2020.

Eckerstorfer, M., and Christiansen, H. H.: The" High Arctic Maritime Snow Climate" in Central Svalbard, Arctic, Antarctic, and Alpine Research, 43, 11-21, doi:10.1657/1938-4246-43.1.11, 2011a.

Eckerstorfer, M., and Christiansen, H. H.: Relating meteorological variables to the natural slab avalanche regime in High Arctic Svalbard, Cold Regions Science and Technology, 69, 184-193, doi:10.1016/j.coldregions.2011.08.008, 2011b.

Eckerstorfer, M., and Christiansen, H. H.: Topographical and meteorological control on snow avalanching in the Longyearbyen area, central Svalbard 2006–2009, Geomorphology, 134, 186-196, doi:10.1016/j.geomorph.2011.07.001, 2011c.

Eckerstorfer, M., Vickers, H., Malnes, E., and Grahn, J.: Near-Real Time Automatic Snow Avalanche Activity Monitoring System Using Sentinel-1 SAR Data in Norway, Remote Sensing, 11, 2863, 2019.

Ekker, R.: varsomdata: GitHub, https://github.com/ragnarekker/varsomdata, 2019.

Engeset, R. V., Ekker, R., Humstad, T., and Landrø, M.: Varsom:regobs - A common real-time picture of the hazard situation shared by mobile information technology, International Snow Science Workshop, Innsbruck, Austria, 2018, 1573-1577,

Engeset, R. V., Landrø, M., Indreiten, M., Müller, K., Mikkelsen, O.-A., and Hoseth, K. I. A.: Avalanche warning in Svalbard, Norwegian Water Resources and Energy Directorate, Oslo, Norway, 25, 2020.

Fitzharris, B., and Bakkehøi, S.: A synoptic climatology of major avalanche winters in Norway, Journal of climatology, 6, 431-446, 1986.

Fitzharris, B.: A climatology of major avalanche winters in western Canada, Atmosphere-Ocean, 25, 115-136, 1987.

Førland, E. J., Isaksen, K., Lutz, J., Hanssen-Bauer, I., Schuler, T. V., Dobler, A., Gjelten, H. M., and Vikhamar-Schuler, D.: Measured and Modeled Historical Precipitation Trends for Svalbard, Journal of Hydrometeorology, 21, 1279-1296, doi:10.1175/jhm-d-19-0252.1, 2020.

García-Sellés, C., Peña, J. C., Martí, G., Oller, P., and Martínez, P.: WeMOI and NAOi influence on major avalanche activity in the Eastern Pyrenees, Cold Regions Science and Technology, 64, 137-145, doi:https://doi.org/10.1016/j.coldregions.2010.08.003, 2010.

García, C., Martí, G., Oller, P., Moner, I., Gavaldà, J., Martínez, P., and Peña, J. C.: Major avalanches occurrence at regional scale and related atmospheric circulation patterns in the Eastern Pyrenees, Cold Regions Science and Technology, 59, 106-118, doi:http://dx.doi.org/10.1016/j.coldregions.2009.07.009, 2009.

595   Hancock, H., Prokop, A., Eckerstorfer, M., and Hendrikx, J.: Combining high spatial resolution snow mapping and meteorological analyses to improve forecasting of destructive avalanches in Longyearbyen, Svalbard, Cold Regions Science and Technology, 154, 120-132, doi:https://doi.org/10.1016/j.coldregions.2018.05.011, 2018.

Hancock, H., Eckerstorfer, M., Prokop, A., and Hendrikx, J.: Quantifying seasonal cornice dynamics using a terrestrial laser scanner in Svalbard, Norway, Nat. Hazards Earth Syst. Sci., 20, 603-623, doi:10.5194/nhess-20-603-2020, 2020.

600   Hansen, C., and Underwood, S. J.: Synoptic Scale Weather Patterns and Size-5 Avalanches on Mt. Shasta, California, Northwest Science, 86, 329-341, 2012.

Hanssen-Bauer, I., Solås, M. K., and Steffensen, E.: The Climate of Spitsbergen, Det Norske Meteorologiske Institutt, 40 pp., 1990.

Hanssen-Bauer, I., Førland, E., Hisdal, H., Mayer, S., Sandø, A., and Sorteberg, A.: Climate in Svalbard 2100 - a knowledge base for climate adaptation., Norwegian Centre for Climate Services1/2019, 207, 2019.

605   Hersbach, H., Bell, B., Berrisford, P., Hirahara, S., Horányi, A., Muñoz-Sabater, J., Nicolas, J., Peubey, C., Radu, R., Schepers, D., Simmons, A., Soci, C., Abdalla, S., Abellan, X., Balsamo, G., Bechtold, P., Biavati, G., Bidlot, J., Bonavita, M., De Chiara, G., Dahlgren, P., Dee, D., Diamantakis, M., Dragani, R., Flemming, J., Forbes, R., Fuentes, M., Geer, A., Haimberger, L., Healy, S., Hogan, R. J., Hólm, E., Janisková, M., Keeley, S., Laloyaux, P., Lopez, P., Lupu, C., Radnoti, G., de Rosnay, P., Rozum, I., Vamborg, F., Villaume, S., and Thépaut, J.-N.: The ERA5 global reanalysis, Quarterly Journal of the Royal Meteorological Society, n/a, doi:10.1002/qj.3803, 2020.

610   Isaksen, K., Nordli, Ø., Førland, E. J., Łupikasza, E., Eastwood, S., and Niedźwiedź, T.: Recent warming on Spitsbergen—Influence of atmospheric circulation and sea ice cover, Journal of Geophysical Research: Atmospheres, 121, 11,913-911,931, doi:10.1002/2016JD025606, 2016.

Käsmacher, O., and Schneider, C.: An objective circulation pattern classification for the region of Svalbard, Geografiska Annaler: Series A, 615   Physical Geography, 93, 259-271, doi:10.1111/j.1468-0459.2011.00431.x, 2011.

Keylock, C. J.: The North Atlantic Oscillation and snow avalanching in Iceland, Geophysical Research Letters, 30, n/a-n/a, doi:10.1029/2002GL016272, 2003.

LaChapelle, E. R.: The fundamental processes in conventional avalanche forecasting, Journal of Glaciology, 26, 75-84, 1980.

Laska, M., Grabiec, M., Ignatiuk, D., and Budzik, T.: Snow deposition patterns on southern Spitsbergen glaciers, Svalbard, in relation to 620   recent meteorological conditions and local topography, Geografiska Annaler: Series A, Physical Geography, 99, 262-287, doi:10.1080/04353676.2017.1327321, 2017.

López-Moreno, J. I., Boike, J., Sanchez-Lorenzo, A., and Pomeroy, J. W.: Impact of climate warming on snow processes in Ny-Ålesund, a polar maritime site at Svalbard, Global and Planetary Change, 146, 10-21, doi:https://doi.org/10.1016/j.gloplacha.2016.09.006, 2016.

625   Małecki, J.: Glacio− meteorology of Ebbabreen, Dickson Land, central Svalbard, during 2008–2010 melt seasons, Polish Polar Research, 36, 145-161, doi:10.1515/popore−2015−0010, 2015.

Martin, J.-P., and Germain, D.: Large-scale teleconnection patterns and synoptic climatology of major snow-avalanche winters in the Presidential Range (New Hampshire, USA), International Journal of Climatology, 37, 109-123, doi:10.1002/joc.4985, 2017.

McClung, D.: The Elements of Applied Avalanche Forecasting, Part II: The Physical Issues and the Rules of Applied Avalanche Forecasting, 630   Natural Hazards, 26, 131-146, doi:10.1023/a:1015604600361, 2002b.

McClung, D. M.: The effects of El Niño and La Niña on snow and avalanche patterns in British Columbia, Canada, and central Chile, Journal of Glaciology, 59, 783-792, doi:10.3189/2013JoG12J192, 2013.

Muckenhuber, S., Nilsen, F., Korosov, A., and Sandven, S.: Sea ice cover in Isfjorden and Hornsund, Svalbard (2000–2014) from remote sensing data, The Cryosphere, 10, 149-158, doi:10.5194/tc-10-149-2016, 2016.

635   Niedźwiedź, T.: The atmospheric circulation, in: Climate and Climate Change at Hornsund, Svalbard, edited by: Marsz, A. A., and Styszyńska, A., Gdynia Maritime Univsersity, Gdynia, Poland, 57-74, 2013.

Nordli, Ø., Wyszyński, P., Gjelten, H. M., Isaksen, K., Łupikasza, E., Niedźwiedź, T., and Przybylak, R.: Revisiting the extended Svalbard Airport monthly temperature series, and the compiled corresponding daily series 1898–2018, Polar Research, 39, doi:10.33265/polar.v39.3614, 2020.

640   Onarheim, I. H., Smedsrud, L. H., Ingvaldsen, R. B., and Nilsen, F.: Loss of sea ice during winter north of Svalbard, Tellus A: Dynamic Meteorology and Oceanography, 66, 23933, doi:10.3402/tellusa.v66.23933, 2014.

Peeters, B., Ønvik Pedersen, Å., Loe, L. E., Isaksen, K., Veiberg, V., Stien, A., Kohler, J., Gallet, J.-C., Aanes, R., and Hansen, B.: Spatiotemporal patterns of rain-on-snow and basal ice in high Arctic Svalbard: detection of a climate-cryosphere regime shift, 2019.

645   Rinke, A., Maturilli, M., Graham, R. M., Matthes, H., Handorf, D., Cohen, L., Hudson, S. R., and Moore, J. C.: Extreme cyclone events in the Arctic: Wintertime variability and trends, Environmental Research Letters, 12, 094006, doi:10.1088/1748-9326/aa7def, 2017.

Rogers, J. C., Yang, L., and Li, L.: The role of Fram Strait winter cyclones on sea ice flux and on Spitsbergen air temperatures, Geophysical Research Letters, 32, doi:https://doi.org/10.1029/2004GL022262, 2005.

650 Schauer, A. R., Hendrikx, J., Birkeland, K. W., and Mock, C. J.: Synoptic atmospheric circulation patterns associated with deep persistent slab avalanches in the western United States, Nat. Hazards Earth Syst. Sci. Discuss., 2020, 1-30, doi:10.5194/nhess-2020-302, 2020.

Schweizer, J., Bruce Jamieson, J., and Schneebeli, M.: Snow avalanche formation, Reviews of Geophysics, 41, doi:https://doi.org/10.1029/2002RG000123, 2003a.

655 Schweizer, J., Kronholm, K., and Wiesinger, T.: Verification of regional snowpack stability and avalanche danger, Cold Regions Science and Technology, 37, 277-288, doi:https://doi.org/10.1016/S0165-232X(03)00070-3, 2003b.

Schweizer, J., Kronholm, K., Jamieson, J. B., and Birkeland, K. W.: Review of spatial variability of snowpack properties and its importance for avalanche formation, Cold Regions Science and Technology, 51, 253-272, doi:https://doi.org/10.1016/j.coldregions.2007.04.009, 2008.

660 Schweizer, J., Mitterer, C., Techel, F., Stoffel, A., and Reuter, B.: On the relation between avalanche occurrence and avalanche danger level, The Cryosphere, 14, 737-750, doi:10.5194/tc-14-737-2020, 2020.

Serreze, M. C., Crawford, A. D., and Barrett, A. P.: Extreme daily precipitation events at Spitsbergen, an Arctic Island, International Journal of Climatology, 35, 4574-4588, doi:10.1002/joc.4308, 2015.

van Pelt, W. J. J., Kohler, J., Liston, G. E., Hagen, J. O., Luks, B., Reijmer, C. H., and Pohjola, V. A.: Multidecadal climate and seasonal snow conditions in Svalbard, Journal of Geophysical Research: Earth Surface, 121, 2100-2117, doi:10.1002/2016jf003999, 2016.

665 Vikhamar-Schuler, D., Isaksen, K., Haugen, J. E., Tømmervik, H., Luks, B., Schuler, T. V., and Bjerke, J. W.: Changes in winter warming events in the Nordic Arctic region, Journal of Climate, 29, 6223-6244, doi:10.1175/jcli-d-15-0763.1, 2016.

Vogel, S., Eckerstorfer, M., and Christiansen, H.: Cornice dynamics and meteorological control at Gruvefjellet, Central Svalbard, The Cryosphere, 6, 157-171, doi:10.5194/tc-6-157-2012, 2012.

Walczowski, W., and Piechura, J.: Influence of the West Spitsbergen Current on the local climate, International Journal of Climatology, 31,
670 1088-1093, doi:10.1002/joc.2338, 2011.

Wickström, S., Jonassen, M. O., Vihma, T., and Uotila, P.: Trends in cyclones in the high-latitude North Atlantic during 1979–2016, Quarterly Journal of the Royal Meteorological Society, n/a, doi:10.1002/qj.3707, 2019.

Wickström, S., Jonassen, M. O., Cassano, J. J., and Vihma, T.: Present Temperature, Precipitation and Rain-on-Snow Climate in Svalbard, Journal of Geophysical Research: Atmospheres, n/a, e2019JD032155, doi:10.1029/2019jd032155, 2020.

675 Yarnal, B.: Synoptic Climatology in Environmental Analysis: a Primer, Studies in Climatology Series, edited by: Gregory, S., Bellhaven Pess, London, UK, 1993.

Appendix A: Composite parameter field anomalies by synoptic type

Composite daily air temperature anomaly (°C)
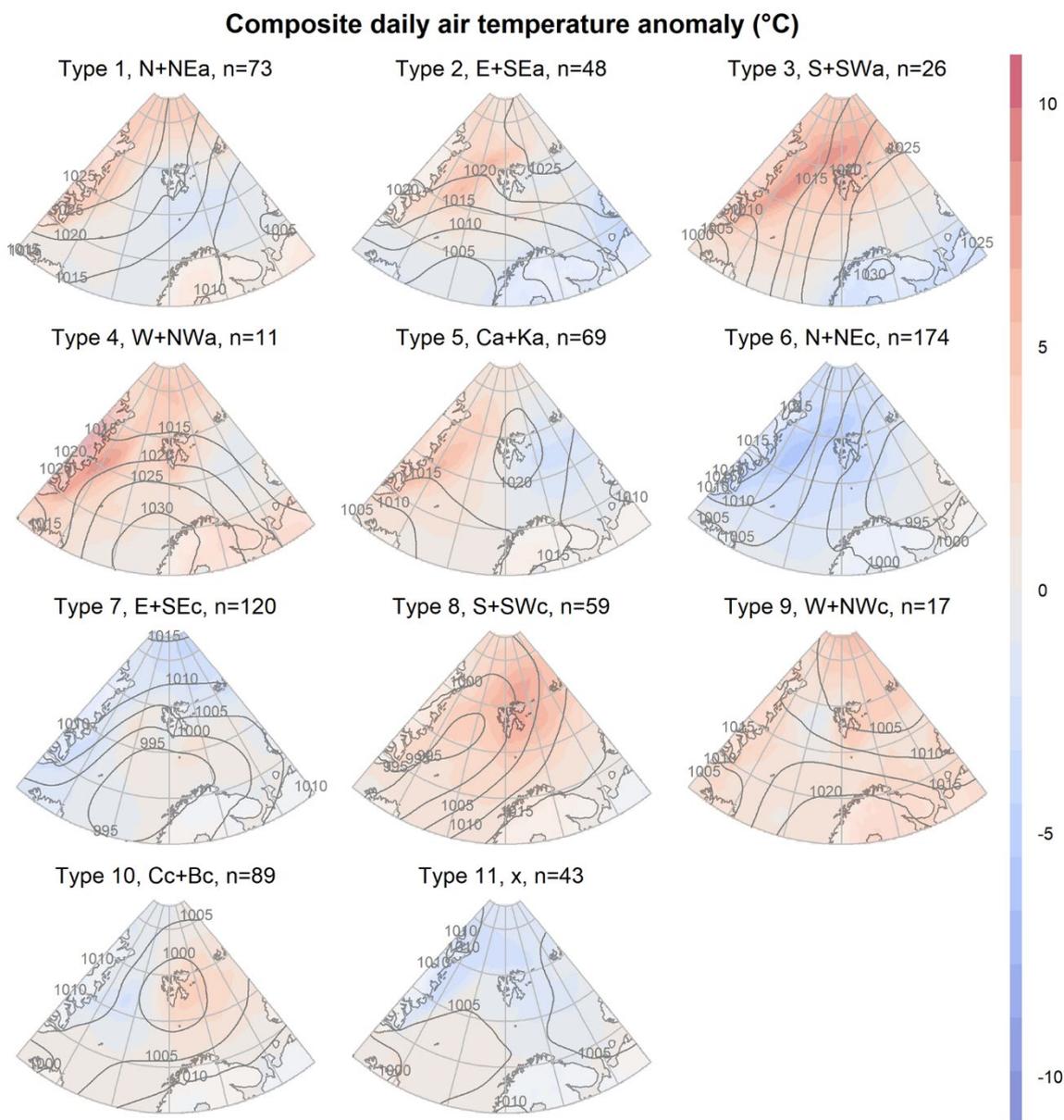
680

Figure A1: Composite daily mean air temperature anomaly by synoptic type, calculated versus mean daily air temperature conditions (Fig. B1). Composite MSLP isobars by synoptic type are included for reference.
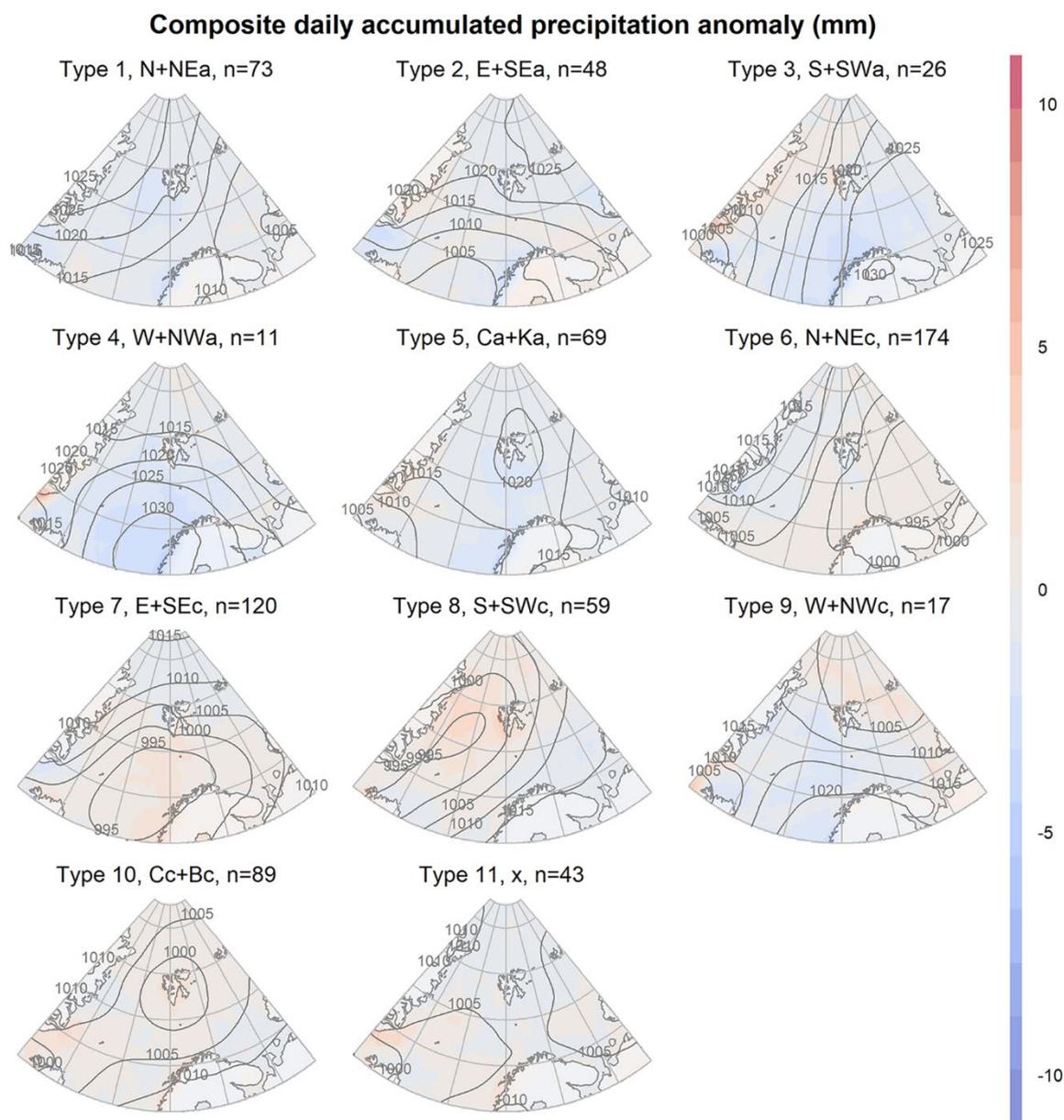
Figure A2: Composite daily accumulated precipitation anomaly by synoptic type, calculated versus mean daily accumulated precipitation conditions (Fig. B2). Composite MSLP isobars by synoptic type are included for reference.
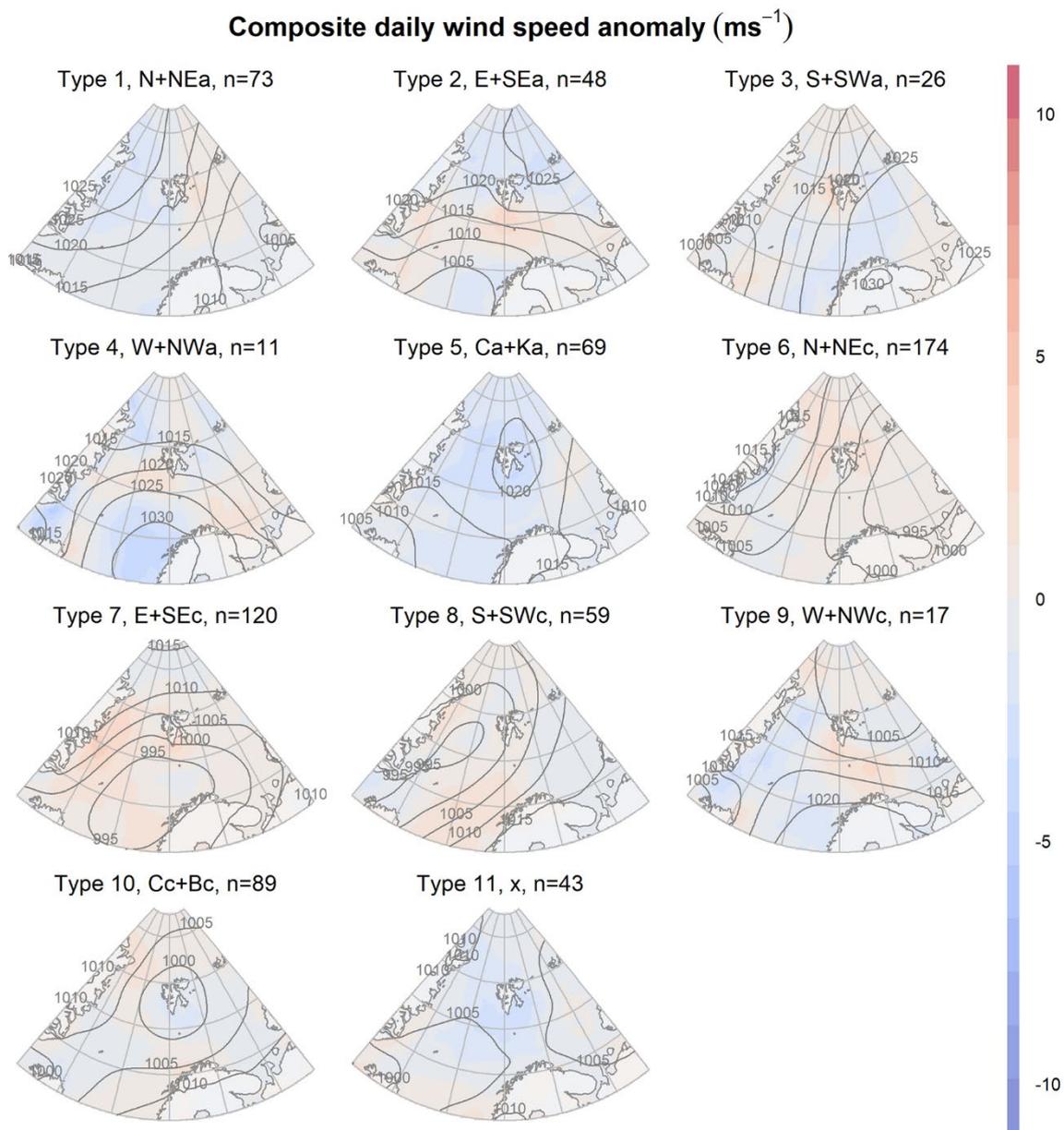
690   **Figure A3: Composite daily mean wind speed anomaly by synoptic type, calculated versus mean daily wind speed conditions (Fig. B3). Composite MSLP isobars by synoptic type are included for reference.**

Appendix B: Composite mean winter condition fields
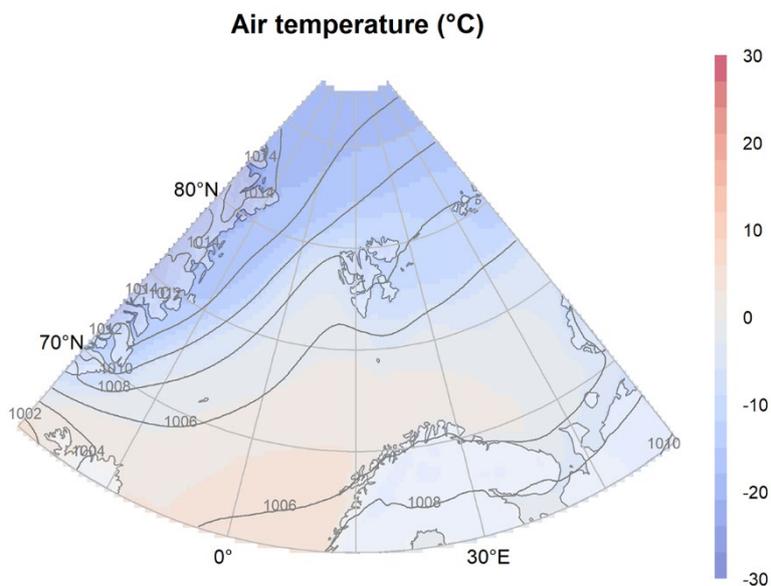
Figure B1: Mean daily air temperature composite field for all winter days (n=729) included in these analyses. This represents the mean daily air temperature conditions from which anomalies are calculated. Composite MSLP isobars for all winter days are included for reference.
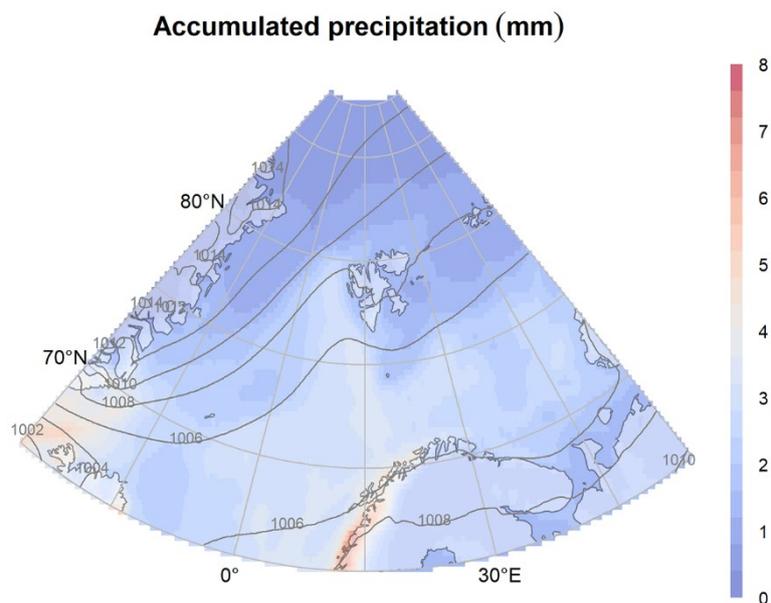
Figure B2: Mean daily accumulated precipitation composite field for all winter days (n=729) included in these analyses. This represents the mean daily accumulated precipitation conditions from which anomalies are calculated. Composite MSLP isobars for all winter days are included for reference.
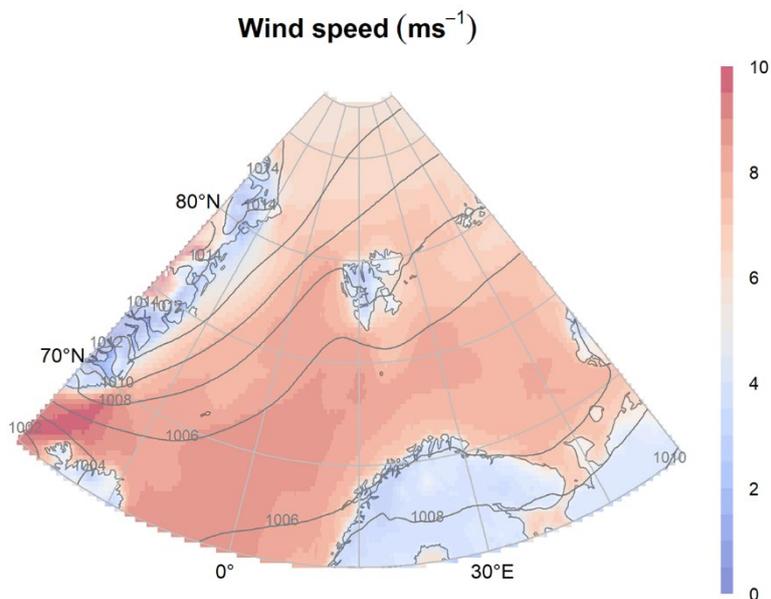
Figure B3: Mean daily wind speed field for all winter days (n=729) included in these analyses. This represents the mean daily wind speed conditions from which anomalies are calculated. Composite MSLP isobars for all winter days are included for reference.

705

Appendix C: Additional composite fields for dry, mixed, and wet avalanche activity
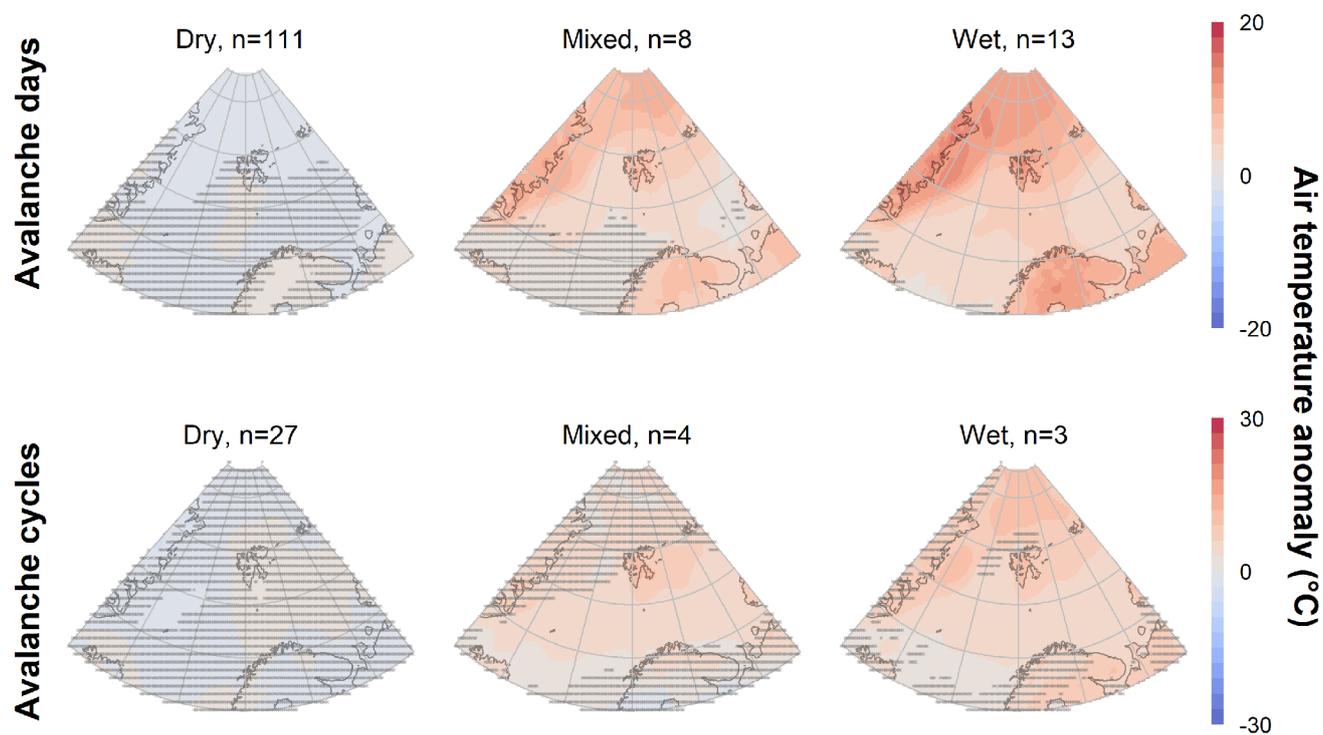
Figure C1: Daily mean air temperature anomalies, relative to mean winter conditions (Fig. B1), for dry, mixed, and wet avalanche days and cycles. Anomalies which are not statistically significantly different from mean winter conditions are indicated with dense hatching.

710
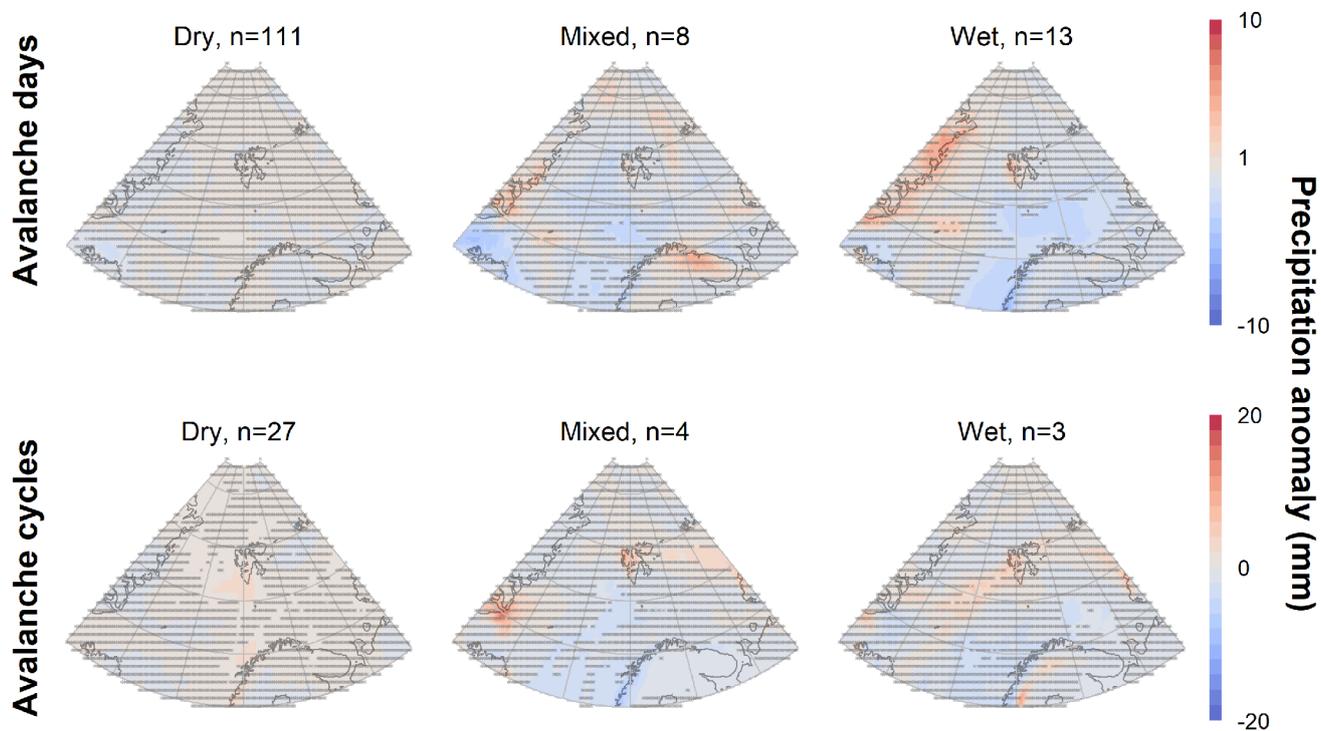
Figure C2: Daily accumulated precipitation anomalies, relative to mean winter conditions (Fig. B2), for dry, mixed, and wet avalanche days and cycles. Anomalies which are not statistically significantly different from mean winter conditions are indicated with dense hatching.
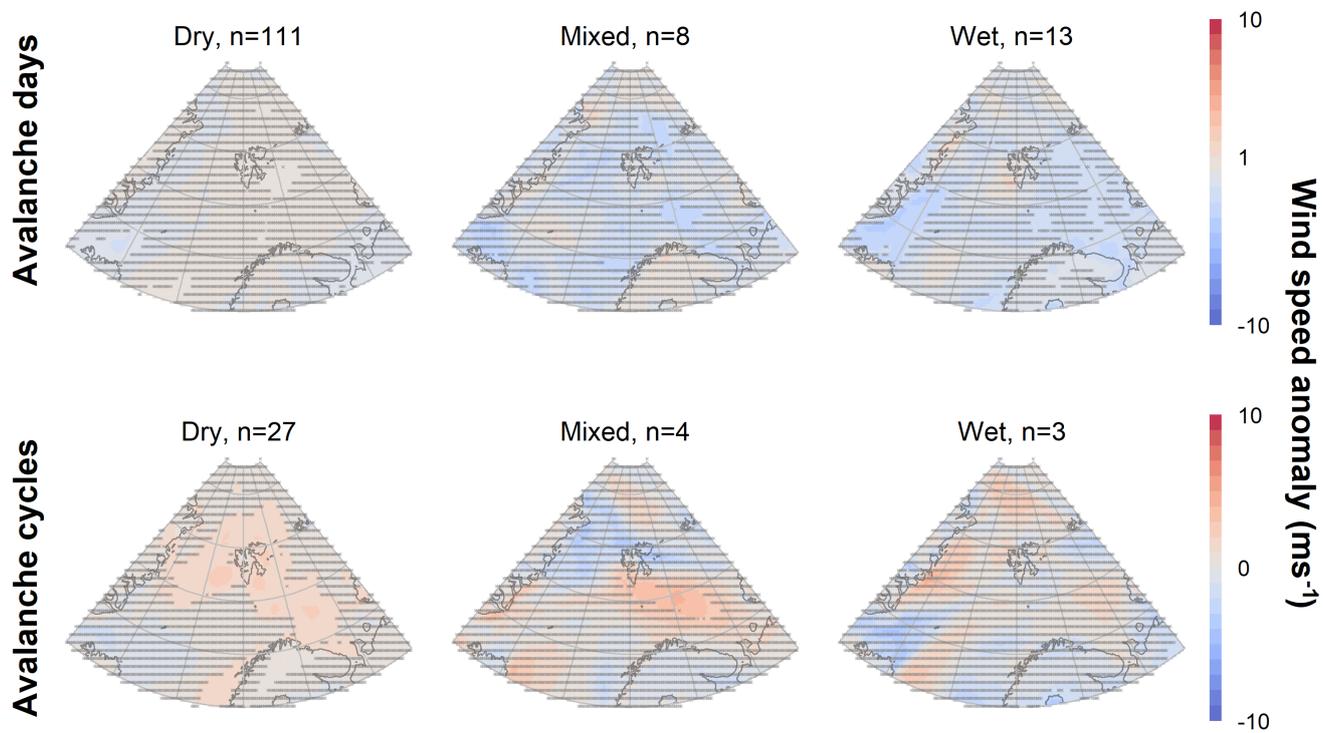
715

Figure C3. Daily mean wind speed anomalies, relative to mean winter conditions (Fig. B3), for dry, mixed, and wet avalanche days and cycles. Anomalies which are not statistically significantly different from mean winter conditions are indicated with dense hatching.